

Worcester Polytechnic Institute Digital WPI

Masters Theses (All Theses, All Years)

Electronic Theses and Dissertations

2002-04-30

Molecular Analysis of Turnip Crinkle Virus Coat Protein Mutations

Ye Zhan

Worcester Polytechnic Institute

Follow this and additional works at: <https://digitalcommons.wpi.edu/etd-theses>

Repository Citation

Zhan, Ye, "Molecular Analysis of Turnip Crinkle Virus Coat Protein Mutations" (2002). *Masters Theses (All Theses, All Years)*. 540.
<https://digitalcommons.wpi.edu/etd-theses/540>

This thesis is brought to you for free and open access by Digital WPI. It has been accepted for inclusion in Masters Theses (All Theses, All Years) by an authorized administrator of Digital WPI. For more information, please contact wpi-etd@wpi.edu.

**MOLECULAR ANALYSIS OF
TURNIP CRINKLE VIRUS COAT PROTEIN MUTATIONS**

**A Thesis
Submitted to the Faculty
of the
WORCESTER POLYTECHNIC INSTITUTE
in partial fulfillment of the requirements for the
Degree of Master of Science
in
Biochemistry
by**

**Ye Zhan
April 2002**

APPROVED:

Dr. Kristin K. Wobbe, Major Advisor

Dr. Craig D. Fairchild, Committee Member

Dr. William D. Hobey, Committee Member

Dr. James P. Dittami, Head of Department

ABSTRACT

TCV (*Turnip crinkle virus*) coat protein is required for the resistance response in *Arabidopsis thaliana* Di-17 plants. An aspartate→asparagine mutation at amino acid four of the coat protein is sufficient to result in resistance-breaking. To determine the essential chemical properties responsible for the induction of resistance, a series of site-directed mutants were produced. Serine as well as asparagine at amino acid four induces systemic disease on both Di-3 and Di-17 plants; however, replacement of aspartate with glutamate retains the ability to induce the HR (hypersensitive response) and resist TCV infection with rapid and strong induction of *PR-I* gene. These data suggest that the negative charge at the fourth amino acid of the coat protein is critical for the induction of resistance. Taken together with other mutagenesis research, the N-terminus of the coat protein appears to be the sole viral recognition element.

The *A. thaliana* TIP protein is suggested to be involved in resistance, mainly through its C-terminus. Interestingly, one of the resistance-breaking mutants (D4N) produces a HR on Di-3 plants that are normally susceptible. The Di-3 TIP protein has several differences from the Di-17 TIP. To detect whether the delayed HR is related to interaction between Di-3 TIP and D4N mutation, a yeast two-hybrid assay was attempted. Interactions have not yet been detected. There are a number of possible explanations.

ACKNOWLEDGEMENTS

I will never forget how hard it was for me during the first year in WPI, I even doubted that if I had chosen the right major. But, after almost two years, I finally finished my master study in Biochemistry. Although I had spent most of my time in GH06 doing my research, I would not be able to make it without the help from these people below.

First of all, I would like to thank my academic advisor Dr. Kristin Wobbe. She is one of the best advisors I have ever seen. She gave me such an interesting project that allowed me getting more familiar with biochemistry. At same time, Kris also gave me so many suggestions that helped me out. Her knowledge, encouragement and patience were important to me, especially when I got frustrated about the negative results. In particular, during the last month, it was her who revised and edited my thesis from time by time with patience. I greatly appreciated her guidance.

I would like to take this opportunity to thank Dr. Craig D. Fairchild and Dr. William D. Hobey for their critical review of my thesis, especially Craig for his kindly gift of yeast host strain and vectors. Thanks for Dr. José Argüello, Dr. Hobey as well as Craig again, for their help to improve my research, suggestions to improve my presentation skills. I enjoyed their discussions in CH560. Also thanks Dr. Daniel G. Gibson III for his help with the microscopic work.

I sincerely thank Frederic Souret, Atin K. Mandal, Katarzyna Galecka and Serdar Gurses, for their assistance, suggestion and discussion in most of my experiments carried out. I appreciate their friendship. I will miss working time with them.

Thanks go to Muslum Akgoz and Thomas M. Hammond for their help and instruction when I set up my research experiments. Muslum was my first teacher in GH06 who helped me get familiar with biochemical techniques, while Tom was my *Arabidopsis* teacher.

I also extend my thanks to Yajuan Zhao, Leanna J. DelGrosso and Cheryl K. Eddins. Their previous outstanding work was the basis for my research project.

Thank all people working in GH06, for giving me a wonderful two-year in biochemical lab. Thank Laurie Smith, Sue Wade and Mary Ballard for their help.

Thank you to Song Wang, Huahui Wu for their friendship and help.

At last, a special thank to Jie Liu, my boyfriend. Thanks for his love, encouragement and support during these two years.

TABLE OF CONTENTS

ABSTRACT	i
ACKNOWLEDGEMENTS	ii
TABLE OF CONTENTS	iv
LIST OF FIGURES AND TABLES	vii
1. INTRODUCTION	1
1.1 A valuable model to investigate interactions between plant and virus --- <i>Arabidopsis thaliana</i> and Turnip crinkle virus (TCV)	1
1.2 Plant resistance responses	3
1.3 <i>R</i> genes, <i>Avr</i> genes and “gene-for-gene” resistance	5
1.4 “Guard hypothesis” and TCV-interacting protein of <i>A. thaliana</i>	8
1.5 TCV coat protein	10
1.6 Pathogenesis-related proteins and <i>PR-I</i> gene	11
1.7 Biochemical properties of amino acid are involved in protein-protein interaction	12
2. METHODS	15
2.1 Plant growth conditions and inoculation	15
2.2 Site-directed mutagenesis for D4E	15
2.3 Site-directed mutagenesis for K9E	16
2.4 Bacterial transformation by electroporation	17
2.5 PRC with bacterial colony-inoculation	17

2.6 DNA mini preparation	18
2.7 DNA maxi preparation	19
2.8 <i>in vitro</i> transcription	20
2.9 RNA extraction from plant tissue	21
2.10 Autofluorescence microscopy	22
2.11 Probe labeling with α - ³² P dCTP	23
2.12 Northern hybridization	23
2.13 Densitometry	24
2.14 Recombinant DBD-Plasmid in the yeast two-hybrid system	24
2.15 Recombinant AD-plasmid in the yeast two-hybrid system	25
2.16 Yeast cell growing conditions and working yeast culture preparation	26
2.17 Yeast competent cells preparation	26
2.18 Yeast co-transformation	27
2.19 β -galactosidase assay	28
3. RESULTS AND DISCUSSION	30
3.1 Analysis of resistance-breaking strains of TCV	30
3.11 N-terminal sequence of the TCV coat protein plays a critical role in recognition	31
3.12 K9E mutation also results in the resistance breaking phenotype on Di-17 plants	33
3.13 Importance of negative charge of the fourth amino acid the coat protein	34

3.13-1 D4S, not D4E, confers the complete resistance-breaking phenotype in Di-17 plants	36
3.13-2 Greater Extent of viral RNA accumulation in susceptible plants	39
3.13-3 <i>PR-I</i> induction was correlated with the phenotype	41
3.2 Detection of interactions between D4N mutant coat protein and <i>Arabidopsis</i> TIP	45
3.21 Analysis of variable infection patterns by D4N	46
3.21-1 Lack of HR-like lesion formation is possibly due to satellite RNA-C	46
3.21-2 Induction of delayed HR-like lesions on both plants	48
3.21-3 Absence of HR-like lesion formation upon <i>in vitro</i> D4N inoculation	50
3.22 Detection of interaction between D4N CP and TIP in a yeast two-hybrid assay	51
4. FUTURE WORK SUGGESTION	56
REFERENCE	58

LIST OF FIGURES AND TABLES

Figure 1-1	Structure of TCV particle	2
Figure 1-2	<i>Arabidopsis thaliana</i> – Di-17	2
Table 1-1	Various types of genetic interactions in “gene-for-gene” model	5
Figure 1-3	Predicted R gene product structures and a model coupling the recognition of microbial Avr-dependent ligand and activation of plant defense	7
Figure 1-4	The “guard hypothesis”	9
Table 3-1	The TCV coat protein mutations	30
Figure 3-1	Schematic representation of TCV genome	31
Figure 3-2	Symptoms of TCV HV-4 and HV-7 infection in <i>A. thaliana</i> and DNA sequencing analysis	32
Figure 3-3	Systemic symptoms of K9E infection in turnip and <i>A. thaliana</i>	33
Figure 3-4	Chemical structures of amino acids involved in the coat protein mutagenesis analysis	34
Figure 3-5	Sequencing analysis of D4E and D4S mutations	36
Figure 3-6	Phenotype of Di-3 plants at 7 dpi	38
Table 3-2	Symptom development and resistance response in <i>A. thaliana</i>	39
Figure 3-7	Phenotype of Di-17 plants at 7 dpi	37
Figure 3-8	Detection of viral RNA accumulation in inoculated plants	40
Figure 3-9	<i>PR-I</i> Northern hybridization	42
Figure 3-10	Relative levels of <i>PR-I</i> in TCV-inoculated <i>A. thaliana</i> plants	43

Figure 3-11	Distinctive phenotype in D4N-infected <i>A. thaliana</i>	46
Figure 3-12	Northern hybridization for <i>PR-1</i>	47
Figure 3-13	Methylene blue stain	47
Figure 3-14	Microscopic examination of TCV inoculated leaves	49
Figure 3-15	Northern hybridization for <i>PR-1</i>	49
Figure 3-16	Northern hybridization for <i>PR-1</i>	50
Table 3-3	Various infection patterns of D4N infection	51
Figure 3-17	Principle of the yeast two-hybrid assay	52
Table 3-4	Description of the plasmids in yeast two-hybrid assay	53
Figure 3-18	Positive β -gal assay	53
Table 3-5	Results of β -galactosidase assay	54

1. INTRODUCTION

1.1 A valuable model to investigate the interactions between plant and virus --- *Arabidopsis thaliana* and *Turnip crinkle virus* (TCV)

Plants constitute the most important group of autotrophic life forms on earth, supplying us with abundant nutritional sources upon which we depend for survival. Unfortunately, our crops are constantly under siege by various pathogens. For instance, rice tungro virus in SE Asia, African casava mosaic virus in Africa and potato viruses in UK result in \$1,500, \$2,000 and \$30-50 millions of dollars per year in losses, respectively (Bustamante and Hull, 1998). However, the use of potent pesticides has not only led to pathogens that are becoming increasingly immune to these chemicals, but also can cause harm to humans and the environment as well. To exploit nonharmful methods, in particular the inherent defense strategies of plants, to prevent or reduce the crop loss by the pathogens would be more beneficial. Thus, scientists in all parts of the world are devoted to studying plant-pathogen models to investigate the molecular basis for disease resistance. *Turnip crinkle virus* (TCV)-*Arabidopsis thaliana* is one such model.

TCV belongs to the *Carmovirus* genus (VC 74.0.2) in *Tombusviridae* family (VC 74) (<http://www.ncbi.nlm.nih.gov/ICTVdb/ICTVdB/74020012.html>). The virion is morphologically icosahedral, composed of 180 coat protein subunits and one molecule of linear positive-sense single-stranded RNA (Figure 1-1). The total genome length is about 4,051-nucleotide (nt). This RNA virus has five open reading

frames encoding proteins which are required for virus replication (p28 and p88), movement (p8 and p9), and encapsidation and movement [coat protein (CP)] (Carrington *et al*, 1989; Hacker *et al*, 1992; White *et al*, 1995). Many plant hosts are susceptible to TCV infection and show varying levels of systemic symptoms, such as mottling, leaf distortion and crinkling, chlorotic lesions and even stunting.

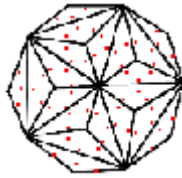


Figure 1-1. Structure of TCV particle
(<http://www.tulane.edu/~dmsander/WWW/335/335Structure.html>)

Arabidopsis thaliana is a plant host capable of supporting TCV replication and spread. It is also a common plant used in laboratory research. *A. thaliana* is a member of the Brassicaceae, along with broccoli and cauliflower (<http://biosci.cbs.umn.edu/labs/dmarks/arabidop.html>). It's relatively small in size with a short life cycle of about 6 weeks, which makes it easy to handle in the lab (Figure 2). It has a small genome compared to other higher plants. Its five chromosomes totally consist of 25,498 genes (The Arabidopsis Genome Initiative, 2000). Furthermore, there are a variety of ecotypes available including *Columbia-0* (Col-0), *Dijon-0* (Di-0), Nössen and others. Different ecotypes may develop different responses when infected by the same pathogen. For instance, Col-0 and Di-3 develop systemic symptoms after TCV invasion, but Di-17 is resistant. This feature, in particular, is



Figure 2. *Arabidopsis thaliana* -Di-17

genetically advantageous. Differences in phenotype may reflect genetic variation. In addition, in the last few years, a large number of mutations in defense responses to pathogens have been identified from *A. thaliana*, such as *npr-1/nim1/sai1*, *etr1* and *cpr*. Investigation of these mutants is beginning to provide insights into the molecular basis of plant defense response.

Taken together, the *A. thaliana* – TCV model has become a valuable model system for investigating the relationships between plant and virus. A thorough understanding of defense mechanisms against pathogens will contribute to improvement of crop yield and human health and to protection of the environment from agricultural pollution.

1.2 Plant resistance responses

Pathogens come from a variety of microorganisms, including some fungi, bacteria and virus species. They invade the plants and cause diseases. The ability to invade the host is a function of their pathogenicity genes whose roles include colonization on the plant surface, formation of haustoria, production of extracellular substances to facilitate invasion (degradation of the plant host cuticle and cell wall), or production of toxins. For instance, the pea pathogen *Fusarium solani* f.sp. *pisi* produces cutinase, an enzyme capable of degrading cutin. Introduction of a cutinase gene enabled *Mycosphaerella*, a wound fungus, to penetrate the intact surface (Lucas, 1998).

In the absence of an effective plant defense, there is a compatible interaction, in which the pathogen successfully multiplies and spreads within the host. The plant eventually becomes systemically diseased and can even die. But in other cases, plants have developed various defense responses. One of these responses is nonhost resistance, in which a series of barriers, such as the cuticle and cell walls, or chemical compounds produced by the plant exclude the pathogen. The leaves of tomato, for example, are covered with sufficient fungitoxic exudates to prevent germination of spores of *Botrytis* (Agrios, 1988). In these cases of nonhost resistance, the plant may not be able to support the growth of the specific pathogen so that the pathogen cannot gain access to the host nutrients and survive. Therefore, the plant will continue to thrive. The second response is known as the active defense response, in which the plant has developed abilities to circumvent pathogen replication and spread. The plant will remain healthy with only limited damage. This strong defense response includes synthesis of anti-microbial enzymes and metabolites, enhanced strengthening of cell walls surrounding the sites of infection, and induction of anti-microbial gene expression (Glazebrook *et al*, 1997).

One of the most prominent features of this active defense response is the hypersensitive response (HR) that has been demonstrated to be effective against fungi, bacteria and viruses. The HR is characterized by necrotic lesion formation at the site of infection (Dempsey *et al*, 1993), and results in isolating the attacking pathogen from the rest of the plant and thus stopping any further spread. The HR has

been observed in some plants such as *A. thaliana*, tobacco and soybean (Dempsey *et al*, 1993; Culver *et al*, 1994; Mohr and Cahill, 2000).

1.3 *R* genes, *Avr* genes and “gene-for-gene” resistance

In many instances, the HR is controlled by a “gene-for-gene” mechanism (Flor, 1971) that involves a direct or indirect interaction between a product (*R*) encoded by a resistance gene of the plant and a corresponding avirulence factor (*Avr*) specified by the pathogen. The *R* gene product recognizes the presence of the *Avr* gene product, allowing elicitation of resistance response. In the absence of the *R* or *Avr* genes, no recognition occurs and the pathogen can infect the host plant and cause disease. Various interactions between plant and pathogen can be described as (Table 1-1):

Table 1-1. Various types of genetic interactions in “gene-for-gene” model.

		Pathogen genotype	
		<i>Avr</i>	<i>avr</i>
Plant genotype	<i>R</i>	Incompatible	Compatible
	<i>r</i>	Compatible	Compatible

The *R* genes are hypothesized to encode proteins that directly or indirectly recognize the specific *Avr* gene products. The predicted characteristics of the *R* proteins include: constitutive expression in healthy, unchallenged plants, enabling plants to detect and defend against pathogen attack; the ability to trigger signaling pathway(s) that initiate the plant defense responses upon the pathogen(s) invasion;

and rapid evolution in readiness for specific pathogen isolates (Hammond-Kosack *et al*, 1997).

The recent cloning of genes for resistance against diverse pathogens from a variety of plants has revealed that many R proteins contain a centrally located nucleotide-binding site (NBS) and a carboxyl-terminal leucine rich repeat (LRR) protein motif (Saraste *et al*, 1990). The NBS – LRR genes have been cloned from a variety of plant species. Sequence analysis of the complete *A. thaliana* genome has identified more than 160 NBS-LRR-encoding genes (The Arabidopsis Genome Initiative, 2000). The NBS motif may serve as an ATP- or GTP-binding site. Within the motif a highly conserved “P-loop” functions in phosphate binding (Traut, 1994). The LRR regions are typically 10~40 repeats of a motif of ~24 amino acids that is highly variable. The LRR domains are implicated in protein-protein interaction and ligand binding (Kobe and Deisenhofer, 1994). Recent research from rice, flax and tomato suggests that the LRR-encoding region is involved in determination of the gene-for-gene interaction specificity (Thomas *et al*, 1997; Ellis *et al*, 1999; Jia *et al*, 2000).

In the *R-Avr* model, similar to receptor-ligand model in human immune system, the R protein is considered the receptor for Avr and the Avr protein is the elicitor of R gene-mediated resistance (Figure 1-3). There are many examples of the correspondence between specific elicitor genes and R genes. In many cases, both the elicitor gene and the corresponding R gene have been cloned. Research with tomato – *Pseudomonas syringae* pv. *tomato* system, for instance, demonstrated that the

avirulent gene *avrPto* conferred resistance to bacterial speck disease in plant cells containing *Pto*. *In vivo* research pointed out the direct interaction between AvrPto and Pto, which was paralleled with AvrPto's ability to induce resistance response (Martin *et al*, 1993; Scofield *et al*, 1996; Tang *et al*, 1996). Similarly, mutagenesis analysis and a yeast two-hybrid assay demonstrated that only AvrPto that interacted with Pto maintained the avirulence activity (Shan *et al*, 2000). Another example is the fungal *Avr* genes *avr4* and *avr9* of *Cladisporium fulvum*. They were indicated to encode proteins that were responsible for elicitation of the HR in tomato plants containing the corresponding *R* genes *Cf-4* and *Cf-9* (Joosten *et al*, 1994).

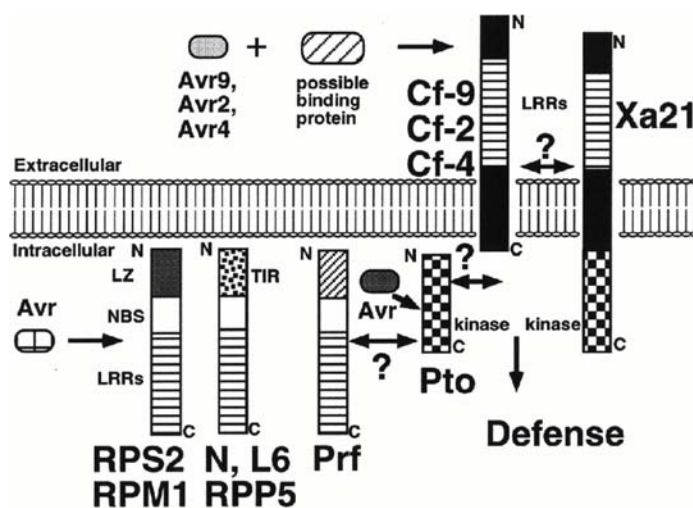


Figure 1-3. Predicted R gene product structures and a model coupling the recognition of microbial Avr-dependent ligand and activation of plant defense. Pto can directly bind AvrPto. The other R proteins probably bind the corresponding Avr gene products, either directly or in association with a binding protein. Both Pto and Xa21 have a protein kinase domain. It is likely that RPM1, RPS2, N, L6, and RPP5 and the Cf proteins also activate defense through a protein kinase. Prf is required for Pto-mediated resistance. Speculative interactions are indicated with a question mark.

Abbreviations: LZ, putative leucine zipper region; TIR, region with homology to the cytoplasmic domain of the Drosophila Toll and human interleukin-1 receptors. LRR, leucine-rich repeat motifs; N, amino terminus; C, carboxyl terminus (Hammond-Kosack and Jones, 1997).

Research with *Arabidopsis* resistance to TCV has also uncovered the involvement of *R – Avr* resistance mechanism. Mutagenesis analysis pointed out that

the TCV CP was the *Avr* factor that conferred resistance in *A. thaliana* Di-17, and a single mutation in the N-terminus of the CP resulted in resistance-breaking (Zhao *et al*, 2000). On the other hand, genetic and biochemical analysis of various *Arabidopsis* ecotypes demonstrated the requirement of a specific dominant gene, namely *HRT* (hypersensitive response to TCV) expression for TCV – induced resistance (Dempsey *et al*, 1997). Strikingly, although no work published to date suggests that there is a direct or indirect interaction between TCV CP and HRT protein, a yeast two-hybrid assay has revealed a physical interaction between the TCV CP and a newly identified *Arabidopsis* protein, TIP (TCV-interacting protein) and demonstrated a correlation between the interaction and TCV-induced resistance (Ren *et al*, 2000). These data suggest the possibility that the resistance activation may be determined by the trilateral interaction among *Arabidopsis* TIP, and HRT as well as the TCV CP. The TCV CP is the elicitor for resistance activation, HRT may be the receptor/effector for the CP, while TIP serves as the essential modulating component that allows the two proteins to functionally link together.

1.4 “Guard hypothesis” and TCV-interacting protein of *Arabidopsis thaliana*

The “gene-for-gene hypothesis” includes direct and indirect interaction between *R* protein(s) and *Avr* factor(s). But evidence of direct interaction is rare. Substantial research led to a modification of the “gene-for-gene hypothesis”, which is referred to as the “guard hypothesis”(van der Biezen and Jones, 1998). In this model, Pto is a general component of host defense, and AvrPto of *P. syringae*

suppresses Pto's function. Prf is an NB-LRR protein that “guards” Pto. When Prf is bound by Pto-AvrPto complex, it activates defense response. Recently, Dangl and Jones (2001) suggested the presence of physical interaction between R proteins and cellular targets of bacterial type III effectors of disease and predicted several mechanistic scenarios: the type III effector initially binds the guard protein and in response, the conformational change increases the affinity of the complex for the R protein, activating resistance (Figure 1-4A). Alternatively, the R protein constitutively forms a complex with its guard protein; interaction of type III effector and the guard induces disassembly and activation of the R protein (Figure 1-4B).

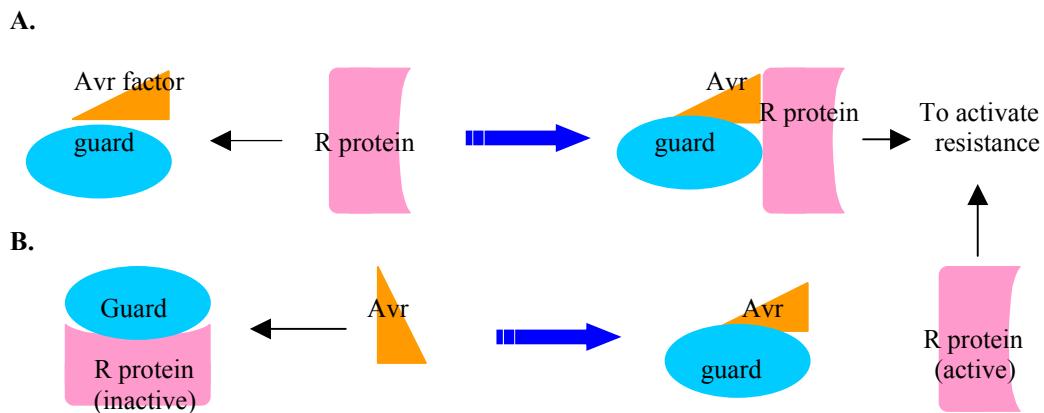


Figure. 1-4 The guard hypothesis (Modified from Dangl and Jones, 2001)

This “guard hypothesis” may explain the TCV CP-induced resistance by *A. thaliana*. TIP - binding to the TCV CP may be the initiating event in the *Arabidopsis* defense pathway to TCV. It is possible that the TIP or the TIP-R protein complex is the cellular target for the CP, and binding to the CP results in disassociation and

activation of the R protein in *A. thaliana*. The mutant CP loses the binding ability and consequently cannot trigger a resistance response.

TIP consists of 451 amino acids, belonging to the NAC family. More interesting about TIP is that it shows transcriptional activity in a yeast two-hybrid assay, which suggests its potential function in activation of defense-related genes. The CP binding site to TIP has been identified as the N-terminal 25 amino acids. And the domain of TIP that binds to the CP was located within a 100 amino acid region in the C-terminus (Ren *et al*, 2001). Furthermore, *TIP* gene comparison between Col-0 and Di-17 indicated that these two genes were identical except for an A→G change in the first intron. The identity of the two plant TIPs coincided with identical behavior in a yeast two-hybrid assay. Sequence analysis indicated that *TIP* cDNAs from Di-3 and Di-17 plants contained five changes at the protein level (Hammond and Souret, 2001), mainly located in the middle or C-terminal domain. Whether these variations in *TIP* are involved in differential responses in susceptible or resistant plants after TCV invasion has not yet been elucidated.

1.5 TCV coat protein

The TCV CP consists of three domains and one arm: the R-domain (N-terminus, internal), the S-domain (shell), an arm and the P-domain (C-terminus, projected) (Hogel *et al*, 1986; Sorger *et al*, 1986). The R-domain is an RNA binding domain joined to the adjacent S-domain, while the P-domain projects from the surface of the capsid and is connected with the S-domain by a hinge region. Both the

S- and P-domains are involved in dimerization (<http://www.vir.gla.ac.uk/staff/bhellad/virusstructureoverview.html>).

However, the importance of the CP reaches far beyond encapsidation. Mutagenesis experiments performed on the TCV CP (Hacker *et al*, 1992; Heaton *et al*, 1991) demonstrated that a functional CP was necessary for virus cell-to-cell and systemic movement. As discussed above, in some host plants the CP serves as the Avr factor to elicit “gene-for-gene” resistance response (Zhao *et al*, 2000; Ren *et al*, 2000). Furthermore, the CP is also involved in sat C-associated symptom modulation (Wang *et al*, 1999).

1.6 Pathogenesis-related proteins and *PR-1*

Research published to date suggests that salicylic acid (SA) plays an important signaling role in resistance that plants develop to pathogens, including fungi and bacteria, as well as viruses. Resistance responses trigger the induction of various novel proteins, referred to as “pathogenesis-related proteins” (PRs). These PR proteins can be induced dramatically in the host plant under pathological or related situations. Moreover, they not only accumulate locally in the infected leaves, but are also induced systemically. Systemic expression of *PRs* is associated with the development of systemic acquired resistance (SAR) against further infection by fungi, bacteria and viruses (van Loon *et al*, 1999). In general, *PR* induction is considered a hallmark of SAR.

At least 14 *PR* families have been identified from various plants, including tobacco, *Arabidopsis* and tomato (van Loon, 1997). Research data have indicated that SA-induced anti-fungal activity is partially due to the anti-microbial activity of some members of the *PR* families. For example, tobacco β -1,3-glucanase (PR-2) (Antoniw *et al*, 1980) and chitinase type I and II (PR-3) (van Loon *et al*, 1982) degrade fungal cell walls. Thaumatin-like protein (PR-5) is a cysteine-rich protein that has anti-fungal activity *in vitro* (van Loon *et al*, 1997). On the other hand, however, so far, no effect of *PRs* against bacteria or viruses has been identified.

PR-1, discovered in 1970, is a dominant group of *PR* families and commonly used as a marker for SAR. PR-1 proteins consist of a few members; at least 4 of them were identified from *Arabidopsis* (van Loon *et al*, 1999). Induction of the *PR-1* gene has been observed in several plant species (van Wees *et al*, 2000; Yalpani *et al*, 2001). The biological functions of *PR-1* are not yet clear.

1.7 Biochemical properties of amino acids are involved in protein-protein interaction

The “gene-for-gene hypothesis” suggests protein-protein interactions. Protein-protein interaction/ recognition is one of the most crucial events for living organisms. It is significant for antigen-antibody recognition, signal transduction, transformation of genetic information into cellular functions (DNA replication, RNA transcription and protein translation as well) and so on. For instance, living organisms receive various stimuli from their environment. They have to detect these

changes and respond appropriately. Such sophisticated responses are under the control of a series of signal transduction pathways, which are mediated by protein-protein interaction via specific protein domains.

In the TCV-induced *Arabidopsis* resistance, the recognition of the CP by the *A. thaliana* R protein is initial and critical. Failure of recognition leads to a compatible interaction. The N-terminus of the TCV CP and the C-terminus of TIP have been demonstrated to be involved in the interaction. Mutational analysis demonstrated that an Asp→Asn mutation at the fourth amino acid of the TCV CP (D4N) resulted in a resistance-breaking phenotype in Di-17 plants (Zhao *et al*, 2000) and failure of protein interactions in yeast cells (Ren *et al*, 2000). How could such a small change in the protein be capable of impeding the interaction? D4N mutation also induced delayed HR-like lesion formation in symptomatic Di-3 plants, which was absent in symptomatic Di-17 plants (DelGrosso, 2000). What is the possible explanation for this disparity? It is well known that the proteins' interaction depends on the chemical properties of the amino acids that constitute the binding or interacting domains. Amino acid substitution in the binding domain may change the protein conformation and affect the binding affinity. D4N may impede the interaction between the CP and the R protein that is responsible for resistance-breaking in Di-17. Further, the different responses developed in Di-3 and Di-17 plants upon D4N inoculation might be associated with the amino acid differences between the Di-3 TIP and Di-17 TIP proteins. Presumably, the Asp→Asn change might make the CP more likely to be recognized by the Di-3 TIP, or the

conformation of the Di-3 TIP might enhance its binding affinity for D4N mutation, contributing to the HR-like lesion formation in Di-3 plants.

2. METHODS

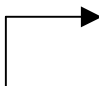
2.1 Plant growth conditions and inoculation

Arabidopsis thaliana lines Col-0, Di-3 and Di-17 were grown in Percival Scientific AR-60L growth chambers under a 14h: 10h day/ night at 22°C. The soil was Pro-Mix BX (Premier Horticulture Inc., Red Hill, PA). The four oldest leaves of each *A. thaliana* plant were inoculated at 21 days post-planting (dpp). The source of TCV inoculum was total RNA isolated from uninoculated leaves of corresponding TCV-infected *A. thaliana* plants or turnips and quantified on denaturing formaldehyde gel. All inoculation used normalized amount of the above extracted RNA to inoculate *A. thaliana* at approximately 0.1ug/ ul RNA. For the mock inoculation, 1× inoculation buffer (50mM glycine, 30mM K₂HPO₄ and 1% celite) was used. Droplets were rubbed across the leaf surface with a glass rod.

2.2 Site-directed mutagenesis for D4S

The template for creating the mutation was pT1d1ΔI (Heaton *et al*, 1989; Akgoz *et al*, 2001). Two primers were designed to introduce both a point mutation at amino acid four of the coat protein (nt 2752) and a new restriction site, *Xho* I, by engineering a silent mutation at the amino acid level. The primers were named D4S-1 (5' AATGGAAAATAGTCCTCGAGTCCGGAAGTTCGCATCTG 3') and D4S-2 (5' CGGACTCGAGGACTATTTTCCATTTCCAGTGTTGATGC 3'). The PCR

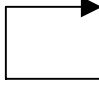
reaction system consisted of 39 ul of dH₂O, 25 µM of each primer, 2 ul of 10mM dNTP mix, 100 ng of pT1d1ΔI, 5 ul of 10× *PfuTurbo* cloned buffer and 2.5 U of *PfuTurbo* polymerase (Stratagene, La Jolla, LA). The total reaction volume was 50 ul. The following parameters were used:

20×		95°C	1 min
		95°C	30 sec
		55°C	1 min
		68°C	16 min
		68°C	10 min
		4°C	99 hrs

5 ul of PRC reaction product was run on a 1% agarose gel to confirm the presence of the band of the correct size. To the remaining PRC product, 20 units of *Dpn* I (Stratagene, La Jolla, LA) was added. The mixture was mixed gently and incubated at 37°C for 2 hours. 1 ul of *Dpn*I – digested PCR product was transformed into competent *E. coli* cells.

2.3 Site-directed mutagenesis for K9E

Two primers designed to produce the K9E mutation were: K9E-5 (5' CCTCGAGTCCGGGAGTTCGCATCTGATGGC 3') and K9E-3 (5' GCCATCAGATGCGAACTCCCGGACTCGAGG 3'). Mutagenesis procedures were similar to that for D4S mutagenesis with modification to the PCR running parameters as follows:

20×		95°C	1 min
		95°C	30 sec
		65°C	1 min
		68°C	16 min
		68°C	10 min
		4°C	99 hrs

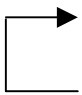
2.4 Bacterial transformation by electroporation

Frozen (- 80°C) *E. coli* DH5α competent cells were thawed on ice. 50 ul of DH5α was used for each transformation, along with 1 ul of *Dpn* I-digested PCR reaction product. GIBCO BRL Electroporation Apparatus (Life Technologies™, Rockville, MD 20849) was used for electroporation and the procedures were carried out following the manual supplied by the manufacturer. 20 ul of each DNA-bacteria mix was used for electroporation and then, incubated in 500 ul of S.O.C. media (2% tryptone, 0.5% yeast extract, 10mM NaCl, 2.5mM KCl, 10mM MgCl₂, 10mM MgSO₄, 20mM glucose) at 37°C for 1 hr with shaking at about 200 rpm. The incubated mixture was briefly centrifuged and some amount of supernatant was removed. The pellet was resuspended in less than 100 ul of remaining supernatant and placed on the LB plus 100 ug/ml ampicillin plates. The plates were incubated at 37°C for 16 hrs.

2.5 PCR with bacterial colony-inoculation

The PCR reaction system consisted of 10 mM dNTP mix, a stock solution of 10× *Taq* buffer, *Taq* polymerase (New England BioLabs® Inc, Beverly, MA 01915),

dH₂O and the corresponding two primers as well. This stock solution was aliquoted into PRC tubes, each of which contained 15 ul of solution. Each tube was inoculated with a colony that formed on the transformed plates. The same colony was also used for DNA mini-preparation. The PCR cycle went as follows:

30×		94°C	1 min
		94°C	30 sec
		55°C	30 sec
		72°C	According to the length of the fragment amplified
		72°C	10 min
		4°C	99 hrs

3 ul of each PRC reaction product was run on a 1% agarose gel to check the presence of a band with the right size.

2.6 DNA mini preparation

A single bacterial colony was transferred into 4 ml of L-broth medium containing 100 ug/ml ampicillin. The culture was incubated 16 hrs at 37°C with shaking (220 rpm). 1.5 ml of overnight culture was transferred into a microfuge tube and centrifuged for 30 seconds. The remaining was stored at 4°C. The pellet was suspended in 100 ul of fresh-prepared ice-cold GTE (50mM glucose, 25mM Tris·HCl, pH 8.0, 10mM EDTA, pH 8.0) solution. 200 ul of 0.2M NaOH and 1% SDS (sodium dodecyl sulfate) was added. After being mixed, 150 ul of ice-cold 3M KOAc solution for lysis was added. The contents were gently vortexed and incubated on ice for 3-5 minutes. The tubes were centrifuged for 5 minutes and supernatant was

transferred into a new microfuge tube and 2 volumes of phenol/ chloroform/ isoamyl alcohol (25: 24: 1) were added. The tubes were vortexed and placed on ice for 2 minutes. After centrifugation, the aqueous phase was transferred into another new microfuge tube and 2 volumes of ethanol were added. The tubes were chilled at -20°C for 1 hour. Next, the tubes were centrifuged for 5 minutes and the pellets were resuspended in 30 ul of TE (10mM Tris·HCl, pH 8.0, 1mM EDTA, pH 8.0) buffer containing 1 ul of RNase. The tubes were incubated at 37°C for 30 minutes and then stored at -20°C.

2.7 DNA maxi preparation

One colony was transferred into 100 ml of L-broth medium containing 100 ug/ml of ampicillin and incubated for 16 hrs at 37°C with shaking (220 rpm). The overnight culture was poured into a centrifuge tube and centrifuged at 735×g rpm for 15 minutes at 4°C. The pellet was resuspended in 6 ml of ice-cold GTE solution. 12 ml of 0.2M NaOH and 1% SDS was added. The tubes were mixed and placed on ice for 5 minutes. 8 ml of ice-cold 3M KOAc solution for lysis was added, thoroughly mixed and incubated on ice for 20 minutes. The mixture was poured through cheesecloth into another new centrifuge tube. 14 ml of isopropanol was added and centrifuged at 5,220×g for 10 minutes at 4°C. The pellet was resuspended in 250 ul of TE buffer and transferred into a microfuge tube. 100 ul of 10M NH₄Oac was added (final concentration is about 2M). The tubes were placed on ice for 15 minutes

and centrifuged for 5 minutes. The supernatant was transferred into new microfuge tube and 2 volumes of ethanol were added. The mixture was placed at - 20°C overnight. The tubes were centrifuged for 5 minutes. The pellet was resuspended in 100 ul of TE buffer and 1 ul of RNase and incubated at 37 °C for 30 min. 42.7 ul 5M NaCl, along with 37 ul 30% PEG (polyethylene glycol) and 1.5M NaCl solution was added. The mixture was mixed well and left on ice for 30 min. The tubes were centrifuged and the pellet was resuspended in 100 ul of TE buffer and 100 ul of 2X PK (Proteinase K) buffer, mixed by vortexing. Then the solutions were incubated at 37°C for 30 minutes and then centrifuged. A phenol/ chloroform/ isoamyl alcohol extraction and an ethanol precipitation were performed, respectively. The tubes were centrifuged for 5 min and the pellet was resuspended in 25 ~ 100 ul TE buffer. The final DNA was stored at - 20 °C.

2.8 *In vitro* transcription

Prior to transcription, 20 ug of DNA was linearized with *Xba*I (New England BioLabs[®] Inc, Beverly, MA 01915) digestion. Then a phenol/ chloroform/ isoamyl alcohol extraction and an ethanol precipitation were performed, respectively. The linearized DNA was resuspended in 40 ul of 0.1% DEPC (diethyl pyrocarbonate)-treated water. For *in vitro* transcription reaction, the followings were added to a microfuge tube: 10 ul of 10× transcription buffer, 10mM ATP, CTP, UTP and GTP (10 ul of each NTP), 2 ul of rRNasin (Promega, Madison, WI 53711), 12 ug of

linearized DNA, 8 ul (400 units) of T7 RNA polymerase (New England BioLabs[®] Inc, Beverly, MA 01915) and 0.1% DEPC-treated H₂O. The total reaction volume was 100 ul. The mixture was incubated at 37°C for 2 hours. 1 ul of RQ1 DNase (Promega, Madison, WI 53711) was added and the mixture was incubated for another 15 minutes. 25 ul of 5M NH₄OAc was added and phenol/ chloroform/ isoamyl alcohol extraction and ethanol precipitation were followed. The tubes were centrifuged for 10 minutes and the pellet was resuspended in 100 ul of 0.1% DEPC-treated H₂O. The final transcripts (*in vitro* RNA) were stored at -20°C.

2.9 RNA extraction for plant tissues

The mortars and pestles were cleaned with bleach and rinsed copiously with deionized water. Dry mortars and pestles were covered with foil and placed in the drying oven overnight. When cooling down, the mortars and pestles were wiped with 20% SDS. After dry, they were covered again and placed at -80°C overnight.

Frozen leaves were ground (for turnip, leaves were separated from mid veins and bolts prior to being ground) in pre-cooled mortar in liquid N₂ until powdered. 5-10 ml of fresh-prepared Nuclear acid extraction buffer (10mM Tris·HCl, pH 8.0, 2mM EDTA, pH 8.0, 2% SDS) and equal amount of phenol/ chloroform/ isoamyl alcohol were added. The frozen mixture was incubated in 37 °C water bath until completely thawed. The mixture was then transferred to a sterile centrifuge tube and centrifuged at 1,310×g for 15 min at 4°C. The aqueous layer was carefully

transferred to a new centrifuge tube and equal amount of phenol/ chloroform/ isoamyl alcohol was added. After being vigorously vortexed for 2 minutes, the mixture was centrifuged again. This phenol/ chloroform/ isoamyl alcohol extraction was repeated about 4 times. The total nucleic acids were precipitated with 1/10 V of fresh-prepared 0.1% DEPC-treated 5M NaCl, along with 2 V of ethanol at -20 °C overnight. Next, the mixture was centrifuged at 8,160×g for 20 min at 4 °C and the pellet was resuspended in 400 ul of 0.1% DEPC-treated H₂O. Then, the equal volume of fresh-prepared 0.1% DEPC-treated 4M LiCl was added and the solution was placed on ice for 4 hours. The nucleic acids were collected by centrifugation at 8,160×g for 30 min at 4 °C. The LiCl pellet was resuspended in 400 ul of 0.1% DEPC-treated H₂O. Another overnight ethanol precipitation was followed with 1/10 V of fresh-prepared 0.1% DEPC-treated 5M NaCl. After centrifugation at 8,160×g for 30 minutes at 4°C, the final RNA was resuspended in 100 ~ 200 ul of 0.1% DEPC-treated H₂O and stored at -80 °C.

2.10 Autofluorescence microscopy

Samples were prepared as described in Dempsey *et al.* (1997). In brief, all the leaves were detached at 7 dpi and fixed in 2% formaldehyde, 5% acetic acid and 40% ethanol for 30 minutes. Then the leaves were cleared sequentially in 50% ethanol for one hour and 95% ethanol overnight. HR-associated autofluorescence was examined by using vertical fluorescent microscope (Scientific Instrument

Division, Buffalo, NY 14215). Pictures were taken with Kodak™ GOLD 200 35mm film for color prints at 3-minute exposures with a fluorescent filter set.

2.11 Probe labeling with α -³²P dCTP

The Primer-It® Random Primer Labeling kit (Stratagene, La Jolla, CA) was used for the incorporation of deoxycytidine-5'-triphosphate α -³²P (NEN, Boston, MA) into the probe. In brief, template of PR-1 (Dempsey, *et al*, 1993) was linearized with *Eco*RI and purified with the use of QIAGEN Purification kit (Qiagen, Valencia, CA). Approximately 50 ng of template DNA was used in the labeling reactions. After labeling, Ambion NucAway™ Spin Columns (Austin, TX) were used to purify the probe. Purification procedures were just followed according to the manufacturer's protocol. LS 6500 multi-purpose scintillation counter (BECKMAN) was used for radio-incorporation accounting. Before hybridization, the labeled PR-1 probe was heated in boiling water for 5 minutes for denaturation.

2.12 Northern hybridization

RNA samples were subjected to electrophoresis on formaldehyde gels, transferred to Magnacharge 0.45 Micro nylon membrane (Osmonics, Westborough, MA). After overnight transfer (about 20 hrs), the membranes were stained (0.03 % Methylene-blue, 0.3 M NaOAc) and the pictures were taken. The dye was then removed with multiple washes of dH₂O. Then the RNA was cross-linked to the

membrane, with a Fisher (Pittsburgh, PA) UV cross linker model # FB-UVXL-1000 using the optimum crosslink setting. 1×10^6 cpm/ml of labeled probe was used for hybridization. In brief, the nylon membranes wrapped with nylon mesh were pre-hybridized at 63°C for 2 hours, and then hybridized with α - ^{32}P labeled probe at 63°C overnight. The membranes were washed 2 times with 1×SSC and 0.1%SDS for 15 minutes, 2 times with 0.5×SSC and 0.1%SDS for 15 minutes and 2 times with 0.1×SSC and 0.1%SDS for 15 minutes. The temperature for washing was 63°C. The blots then were exposed to film at - 80°C for two days with intensifying screens. Autoradiography was performed with Kodak X-OMAT AR films. Modified Church buffer (0.5M $\text{NaHPO}_4 \cdot \text{H}_2\text{O}$, 7% SDS, 0.1mM EDTA, 1%BSA) was used as pre-hybridization and hybridization buffer.

2.13 Densitometry

Intensity of ribosomal RNA on the nylon transfer membranes and intensity of labeled PR-1 bands on the blots were measured using 1D Image Analysis Software by Kodak Digital Science (Rochester, NY)

2.14 Recombinant DBD-plasmid in the yeast two-hybrid system

DNA fragments of wild type TCV coat protein or mutant D4N coat protein were amplified from pT1d1ΔI by PCR and inserted into the multiple cloning site of pGBT9 of the *GAL4*-based MATCHMAKER Two-Hybrid System (Clontech, Palo

Alto, CA 94303) to generate DNA-binding domain/ target protein hybrid plasmids. The primers for the coat protein cloning were modified from Lin and Heaton (J. General Virology, 2001). The *EcoRI*-tagged upstream primer CP-5 (5' CTGgaattcGAAAATGATCC 3') and the *BamHI*-tagged downstream primer CP-3 (5' GAggatccACTATTACCGTAC 3') were used to amplify wild type coat protein. The *EcoRI*-tagged upstream primer CP-D4N-5 (5' CGCTGgaattcGAAAATAATCC 3') and the *BamHI*-tagged downstream primer CP-D4N-3 (5' GAggatccACTATTACCGTAC 3') were used to amplify D4N coat protein. Each amplified DNA fragment and pGBT9 plasmid were digested with *EcoRI* and *BamHI* and purified prior to ligation. T4 DNA ligase (New England BioLabs® Inc, Beverly, MA 01915) was used to construct the DNA-binding/ target-protein hybrid plasmids wt-pGBT9 and D4N-pGBT9, respectively.

2.15 Recombinant AD-plasmid in the yeast two-hybrid system

DNA fragments of TIP (TCV-interacting protein) were amplified from *A. thaliana* line Di-3 or Di-17 cDNA by PCR and inserted into the multiple cloning site of pGAD424 of the *GAL4*-based MATCHMAKER Two-Hybrid System (Clontech, Palo Alto, CA 94303) to generate activation domain/ prey-protein hybrid plasmids. The *BamHI*-tagged upstream primer TIP-5 (5' CACGggatccTGAAAGAAGACATG 3') and the *PstI*-tagged downstream primer TIP-3 (5' CGctgcagTGCGACTAGACTG 3') were used to amplify TIP cDNA fragments (TIP cDNA was prepared by Tom Hammond and Frederic Souret). Each amplified cDNA

fragments and pGAD424 plasmid were digested with *Bam*HI and *Pst*I and purified prior to ligation. T4 DNA ligase (New England BioLabs ® Inc, Beverly, MA 01915) was used to construct the activation domain/ prey-protein hybrid plasmids Di3-pGAD424 and Di17-pGAD424, respectively.

2.16 Yeast cell growing conditions and working yeast culture preparation

Yeast cells and corresponding vectors were kindly provided by Dr. Craig Fairchild. First, an inoculum of the frozen stock yeast cells (Y187) was streaked on a fresh YPDA (adenine-supplemented YPD medium, 20g/l of Difco peptone, 10g/l of yeast extract, 0.1g/l of adenine, pH 5.8, 2% dextrose) plate and incubated at 30°C for a couple of days until the yeast colonies grew to a diameter of > 2 mm. A separate colony was picked up, dispersed in 500 ul of autoclaved dH₂O and placed on YPDA and SD(-)Trp/Leu (selective medium without tryptophan and leucine). This was the working culture and the plate was sealed with Parafilm and stored at 4°C for up to 2 months only if there was no colony growing on SD(-)Try/Leu plate. All the yeast cells for the following experiments were propagated from well-isolated colonies of the plate and incubated at 30°C.

2.17 Yeast competent cells preparation (Lithium acetate method)

A single colony was picked up, dispersed in 1 ml of YPDA and transferred to a sterile flask containing 19 ml of YPDA medium. The yeast cells were incubated at

30°C with vigorous shaking (250 rpm) for 16 – 18 hours to the stationary phase ($OD_{600} > 1.5$). Then, an appropriate amount of overnight culture was transferred to 300 ml of YPDA medium to get the OD_{600} between 0.2 – 0.3. 300 ml YPDA culture was incubated at 30°C for 3 hours with 250 rpm shaking. Then the OD_{600} should be 0.5 ± 0.1 . The culture was placed in several 50-ml tubes and centrifuged at $1,000 \times g$ for 5 minutes at room temperature. The cell pellet was resuspended in 25 ml of sterile dH₂O by vortexing. The cell mixture was subjected to a second centrifugation at $1,000 \times g$ for 5 minutes at room temperature. The cell pellet was resuspended in 1.5 ml of freshly prepared, sterile 1×TE/LiAc. The competent yeast cells could be kept in ice up to 1 hour.

2.18 Yeast co-transformation

Yeast co-transformation was performed followed the MATCHMAKER Two-Hybrid System 3 User Manual (Clontech, Palo Alto, CA 94303). A required number of sterile microfuge tubes were set up and a series of materials were added into each tube in the following orders. Prior to adding, the carrier testes DNA was heated in the boiling water for 5 minutes. First, 0.1 ug of each plasmid was added, along with 100 ug of carrier testes DNA to the appropriate tube. Second, 100 ul of the yeast competent cell was added to each tube and well mixed. Then, 600 ul of PEG/LiAc (50% of PEG 4000, 1× TE buffer, 1× LiAc, freshly prepared prior to usage) was added and mixed by vortexing. The mixture was incubated at 30°C for 30 minutes

with 200 rpm shaking. 70 μ l of DMSO (dimethyl sulfoxide) was added to each tube, mixed gently by inversion. The mixture was incubated at 42°C for 15 minutes, followed by ice chill for 2 minutes. Then the cells were centrifuged at 16,000 \times g for 5 seconds at room temperature. The cell pellet was resuspended in 0.5 ml of 1 \times TE buffer. Each transformant was spread onto three plates containing the appropriate medium, i.e., SD(-)Trp, SD(-)Leu and SD(-)Trp/Leu, respectively. The plates were incubated at 30°C until the colonies appeared.

2.19 β -galactosidase assay ----- colony lift filter method

β -galactosidase assay was followed the MATCHAKER Two-Hybrid System manual (Clontech, Palo Alto, CA 94303). Colony lift filter assay was performed using the freshly transformed colonies, 1 – 2 mm in diameter. A piece of sterile Whatman 75mm filter was presoaked in 2.5 ml of Z buffer/X-gal* (5-bromo-4-chloro-3-indoly- β -D-galactopyranoside). Another sterile Whatman 75mm filter was placed over the surface of the agar plate containing the transformant colonies. At least three asymmetric holes were made through the filter into the agar. The filter was carefully lifted and submerged into liquid nitrogen for 10 seconds with colonies facing up. Then the frozen filter was allowed to thaw at room temperature and carefully placed, colony side up, on another filter that was presoaked in Z buffer/X-gal solution, avoiding the air bubbles between the filters. The filters were incubated at 30°C and checked periodically for the appearance of blue colonies.

* Z buffer/X-gal solution [100 ml of Z buffer (16.1 g/l of $\text{Na}_2\text{HPO}_4 \cdot 7\text{H}_2\text{O}$, 5.5 g/l of $\text{NaH}_2\text{PO}_4 \cdot \text{H}_2\text{O}$, 0.75 g/l of KCl and 0.246 g/l of $\text{MgSO}_4 \cdot 7\text{H}_2\text{O}$, pH 7.0), 0.27 ml of β -mercaptoethanol, 1.67 ml of X-gal stock solution (20 mg/ml N, N-dimethylformamide)].

3. RESULTS AND DISCUSSION

3.1 ANALYSIS OF RESISTANCE-BREAKING STRAINS OF TCV

Although Di-17 plants are resistant to TCV, a small subset of TCV-inoculated Di-17 plants occasionally develops a systemic infection. The virus isolated from these systemically infected plants exhibits virulence on Di-17 plants. Resistance-breaking phenomena shown on Di-17 plants indicate the presence of a potential mutant virus that is not recognized by the plant. Chimeric construction analysis (Zhao *et al*, 2000) of such a mutant with wt TCV demonstrated that mutations in the CP (coat protein) of TCV are responsible for resistance-breaking and suggested the CP is the elicitor of resistance by *A. thaliana*. In an effort to determine the range of determinants on TCV recognized by resistant Di-17 plants, a number of resistance-breaking strains were created or isolated (Zhao *et al*, 2000; DelGrosso, 2000; Eddins, 2000), including D4N, P5S, HV-4, HV-6 and HV-7. All the CP mutations involved in site-directed mutagenesis in this thesis were summarized in Table 3-1.

Table 3-1. The TCV coat protein mutations

Mutant	D4N	D4E	D4S	P5S	K9E
Location in CP	4	4	4	5	9
Substitution	Asp→Asn	Asp→Glu	Asp→Ser	Pro→Ser	Lys→Glu

3.11 The N-terminal sequence of the TCV coat protein plays a critical role in recognition

Random mutagenesis had previously been undertaken to identify other regions that might be involved in the resistance-breaking phenomenon; three additional hypervirulent (HV) mutants were identified. The *Bam*HI – *Hind*III region (Figure 3-1) of each mutant that covered the N-terminal sequences of the CP was cloned and inserted into the TCV wild type clone. These chimeric clones were named HV-4, HV-6 and HV-7, respectively (DelGrosso, 2000).

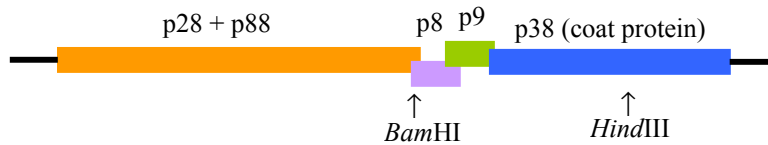


Figure 3-1. Schematic representation of TCV genome with the *Bam*HI – *Hind*III region.

I produce infectious RNA of each of these strains and inoculated both Di-3 and Di-17 plants. When inoculated with *in vivo* TCV HV-4 or HV-7, Di-3 plants showed systemic symptoms at 4 dpi, while Di-17 plants failed to display HR and eventually developed systemic disease at 4-5 dpi. HV-7 seemed more virulent than HV-4 as symptoms appeared earlier and were more severe, with the plants exhibiting a greater degree of chlorosis and stunting (Figure 3-2). Because no systemic symptoms were observed in Di-3 plants inoculated with *in vitro* HV-6 and no virus RNA was detected on the formaldehyde gel, HV-6 was not used for further experiments.

The partial sequencing of HV-4 and HV-7 revealed only one mutation in the CP at protein level (Figure 3-2), i.e., an A→G replacement at 2,767 nt of HV-4 which resulted in a lysine→glutamate change at amino acid nine (K9E) and two consecutive C→A mutations at 2,755 and 2,756 nt on HV-7 that caused proline→asparagine substitution at amino acid five (P5N).




TCV	Symptom appearance	Sequenced portion	Mutations in the CP	Phenotype(11 dpi)
HV-4	5 dpi	2,131-2,806	at 2,767 A→G (Lys→Glu) (K9E)	
HV-7	4 dpi	2,149-2,779	at 2,755 and 2,756 (C→A) (Pro→Asn) (P5N)	
HV-6	NA	NA	NA	

Figure 3-2. Di-17 plants develop the resistance-breaking phenotype upon inoculation with TCV HV-4 and HV-7, respectively. DNA sequencing analysis identifies the mutations in TCV. The picture related to HV-6 is taken from Di-3 plant. The numbers shown in the table identify the nucleotides of TCV (NA: not applicable).

Previously, another mutation at amino acid five of the CP had been identified, in which a C→T transition at 2,755 nt resulted in a proline→serine change (P5S). The P5S mutation was engineered by site-directed mutagenesis and

proved to be responsible for induction of resistance-breaking in Di-17 plants (Zhao *et al*, 2000). It is likely that the P5N mutation may have the similar virulence effect on Di-17 plants, and therefore it was not studied further.

3.12 K9E mutation also results in the resistance-breaking phenotype on Di-17 plants

Sequence analysis of TCV HV-4 revealed in addition to the K9E mutation in the CP, other putative mutations in the movement protein p8. In order to determine if the K9E mutation was responsible for the resistance-breaking phenotype, it was necessary to produce it in a wild type background. The K9E mutation was engineered by site-directed mutagenesis. Its virulence was proved on Di-3 plants and turnips (Figure 3-3). Next, Di-17 plants were inoculated with K9E and as expected, all developed systemic symptoms and no lesion formation was observed (Figure 3-3).



Figure 3-3. Systemic symptoms of K9E infection in turnip (left, 20 dpi), Di-3 (middle, 9 dpi) and Di-17 (right, 9 dpi), respectively.

These results re-emphasize the importance of the CP N-terminus in viral recognition. The N-terminus of the CP (especially the first 25 amino acids) is

thought to bind to an *A. thaliana* protein — TIP; and CP – TIP binding might be the first event in resistance (Ren *et al*, 2000). Presumably, mutations at the N-terminus block viral recognition by interfering with binding to the TIP or another protein such as HRT and therefore break resistance.

3.13 Importance of negative charge at the fourth amino acid of the coat protein

The mutational analysis of the CP raises the question. How is a single mutation in the CP capable of impeding viral recognition resulting in resistance-breaking? An Asp→Asn change is a small change that maintains size and hydrophilicity (Figure 3-4). As is well known, resistance induction like many other cellular processes involves protein – protein interactions. The charges, hydrogen bonding and hydrophobic properties of an amino acid may influence the interaction/recognition of the individual functional groups and the amino acid side chains. We were interested in whether the hydrogen bonding or the charge of the amino acid was involved in breaking interaction between the TCV CP and the R protein in Di-17. Therefore, two TCV mutations, D4E and D4S (Figure 3-4) were engineered to determine which chemical property would be more important (Eddins, 2000).

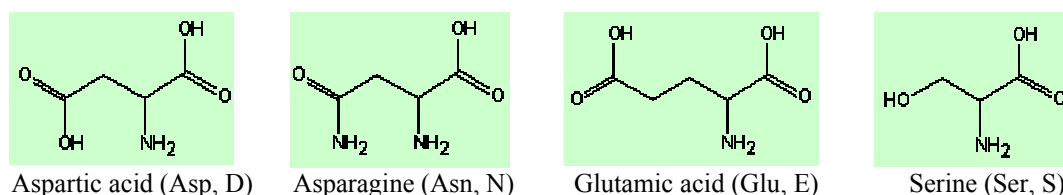


Figure 3-4. Chemical structures of amino acids involved in the coat protein mutagenesis analysis.

D4E and D4S were designed to contain only one substitution in the CP, replacing aspartate (D) with glutamate (E) and serine (S), respectively. D4E and D4S were first used to inoculate turnips and Di-3 plants. The D4E mutant was definitely capable of viral replication and spread, whereas the D4S mutant appeared to lack virulence. DNA sequencing was carried out to analyze whether there were other mutations that would explain lack of disease symptoms of D4S-infected turnips. The sequencing data confirmed the presence of the engineered mutations. However, a single base deletion in D4S at amino acid two of the CP caused a frameshift in the CP. So, the D4S mutation was re-constructed by site-directed mutagenesis using newly designed primers.

Sequence analysis confirmed that D4E contains a T→G replacement at nucleotide 2,754, resulting an Asp→Glu change. In addition, however, there was a G→T substitution at 2,766 nt, which is a silent mutation (Arg→Arg). D4S includes G→A and A→G changes at nucleotide 2,752 and 2,753 that cause an Asp→Ser replacement. A silent A→C substitution at 2,758 nt in D4E and D4S introduced a restriction site. Sequence analysis proved that no additional mutations were found (Figure 3-5). Both D4E and D4S were virulent on turnip and Di-3. These mutants were then used in a series of experiments to investigate the essential chemical properties involved in induction of resistance.

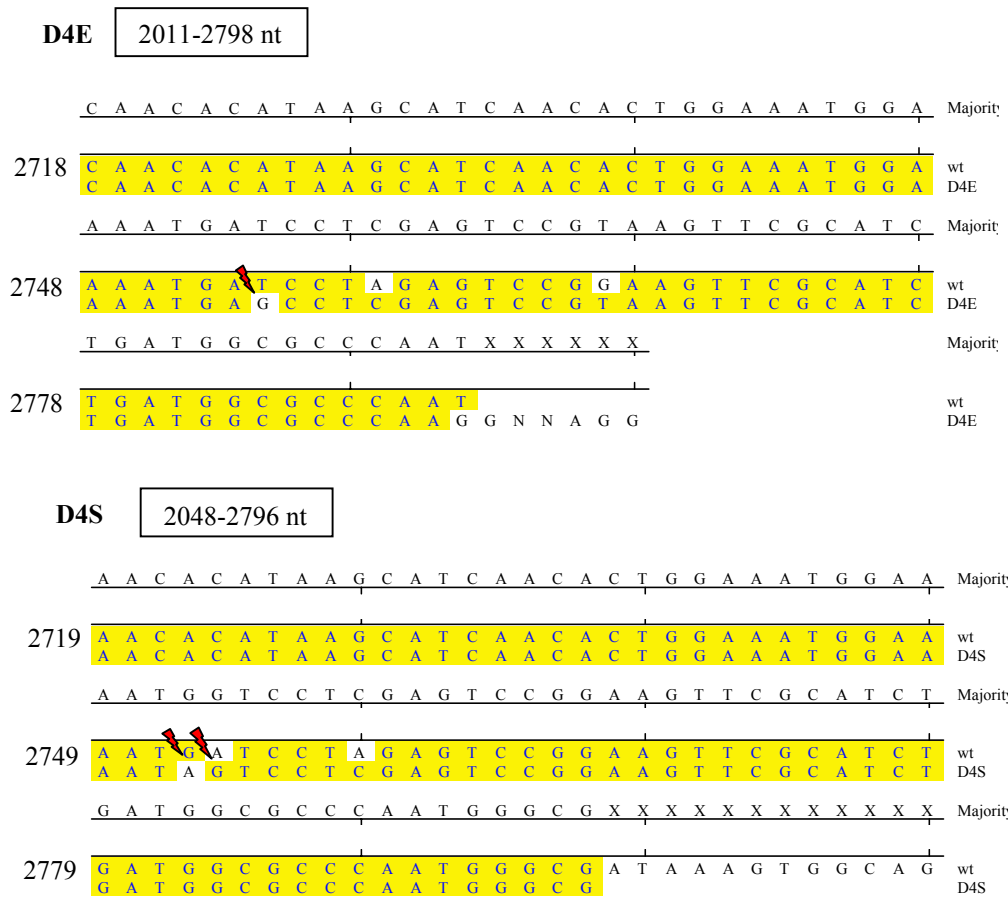


Figure 3-5. Sequencing of D4E and D4S mutations. The rectangles indicate the TCV regions sequenced, and the numbers above identify the nucleotide in TCV.

3.13-1 D4S, not D4E, confers the complete resistance-breaking phenotype in Di-17 plants

Generally, Di-17 plants possess the ability to resist wt TCV infection,

displaying the hypersensitive response (HR) at an early stage. The HR is detected as the tiny brown-yellow spots in the inoculated leaves.

To further understand the molecular basis underlying of viral infection, Di-3 and Di-17 plants were inoculated with D4E and D4S, respectively. All Di-3 plants displayed systemic symptoms (Figure 3-6) and no HR was observed, demonstrating that the viruses were infectious and functional. The inoculated Di-17 plants developed a range of phenotypes (Figure 3-7) dependent on the inoculated virus. D4S-inoculated plants did not display lesions and became systemically infected. The plants were generally smaller in size, reflecting stronger virulence of the virus. In contrast, D4E-inoculated Di-17 plants showed a response similar to wt TCV-inoculated Di-17 plants. More than 80% of D4E-inoculated plants displayed HR in the inoculated leaves and did not become systemically infected during the observation period (7 dpi). A small subset still developed systemic symptoms at 5 – 6 dpi, but this was not significantly different than the number of wt-inoculated plants that developed systemic symptoms. The patterns of symptom development are summarized in Table 3-2.



1	2
3	4

Figure 3-6. Phenotype of

Di-3 plants at 7 dpi.

1.mock inoculation

2.wt-TCV inoculation

3.D4E inoculation

4.D4S inoculation

1	2
3	4

Figure 3-7. Phenotype of
Di-17 plants at 7 dpi.

1. mock inoculation

2. wt-TCV inoculation

3. D4E inoculation

4. D4S inoculation

The small photos inserted
showed HR at 3 dpi.



Table 3-2. Symptom development and resistance response in *A. thaliana* after inoculation with TCV coat protein mutants (up to 14 dpi).

RNA	<i>A. thaliana</i> Di-3			<i>A. thaliana</i> Di-17		
	Symptom Appearance	Percent Systemically Infected	Lesion Formation	Symptom Appearance	Percent systemically Infected	Lesion Formation
WT	~ 4 - 5 dpi	100 %	No	~ 4 – 5 dpi	17 %	~ 3 – 4 dpi
D4E	~ 4 – 5 dpi	100 %	No	~ 5 – 6 dpi	15 %	~ 3 – 4 dpi
D4S	~ 4 – 5 dpi	100 %	No	~ 4 – 5 dpi	100 %	No

The disparity of phenotype upon D4E- or D4S-inoculation further suggests that a negatively charged amino acid at amino acid four is required for the interaction with TIP or HRT protein in Di-17 plant.

3.13-2 The extent of viral RNA accumulation in susceptible plants was greater in the uninoculated leaves

Viral RNA accumulation detected by formaldehyde denaturing gel indicated the correlation between phenotype and virus spread in plants. In the symptomatic plants (Figure 3-8, b-e, i-j), either Di-3 or Di-17, viral RNA could be detected by methylene blue stain in the inoculated leaves at 3 dpi. Viral RNA accumulation continued during the observation period (7dpi) and also spread systemically to the uninoculated leaves by 7 dpi. Viral RNA accumulation was not observed in the uninoculated leaves at 3 dpi, demonstrating lack of significant replication by this time.

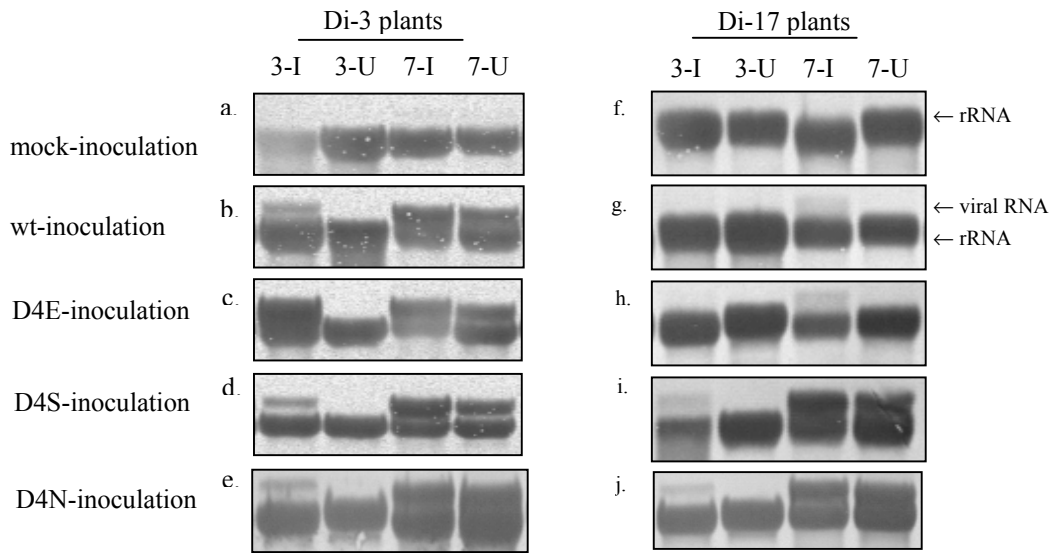


Figure 3-8. Methylene blue stain for detection of viral RNA accumulation in inoculated plants. 3 - 3 dpi; 7 - 7 dpi; I - inoculated leaves; U - uninoculated leaves.

In the wt- or D4E-inoculated Di-17 plants that developed HR and became systemically resistant, the pattern of viral RNA accumulation was different from that observed in the systemically diseased plants. By methylene blue stain, no obvious viral RNA accumulation was detected at 3 dpi. Though viral RNA was observed in the inoculated leaves at 7 dpi, none was seen in the uninoculated leaves at this time, consistent with lack of symptoms in these leaves (Figure 3-8, g-h) and the clear induction of the HR. D4S-inoculated Di-17 plants displayed viral RNA accumulation patterns very similar to Di-3 inoculated plants, with viral RNA visible in the inoculated leaves at 3 dpi and present in the uninoculated leaves by 7 dpi.

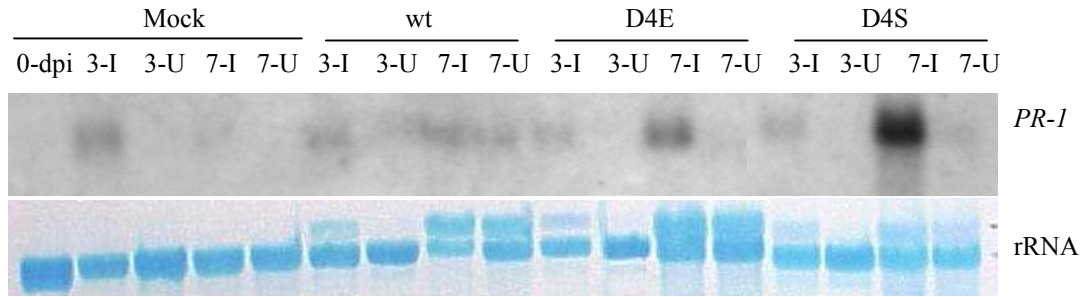
3.13-3 *PR-1* induction was inversely correlated with resistance-breaking

A Di-17 plant typically responds to wt TCV infection with both development of HR and activation of SAR. Failure to induce the HR and SAR in Di-3 plants results in systemic disease. A hallmark of SAR activation is the strong induction of *PR-1* mRNA accumulation (Dempsey *et al*, 1993; van Loon and van Strien, 1999; Wong, *et al*, 2002).

With a single amino acid mutation at amino acid four of TCV CP, D4S induced resistance-breaking in Di-17, whereas D4E maintained the ability to develop the HR and to trigger defense responses. To determine whether the resistance-breaking phenotype was associated with the lack of induction of *PR* genes, induction of *PR-1* gene on both Di-3 (Figure 3-9a) and Di-17 plants (Figure 3-9b) by TCV mutants was monitored.

In mock-inoculated plants, the levels of *PR-1* mRNA in Di-3 and Di-17 plants generally were undetectable, with the exception of low levels seen in mock-inoculated leaves at 3 dpi, presumably caused by mechanical inoculation (Dempsey *et al*, 1993). In wt-inoculated Di-17 plants, rapid and systemic induction of *PR-1* was monitored at relatively high level, and the uninoculated leaves showed *PR-1* level equivalent to the inoculated leaves at 7 dpi, which was consistent with other studies (Dempsey *et al*, 1993; Wong *et al*, 2002).

a. Di-3 plants



b. Di-17 plants

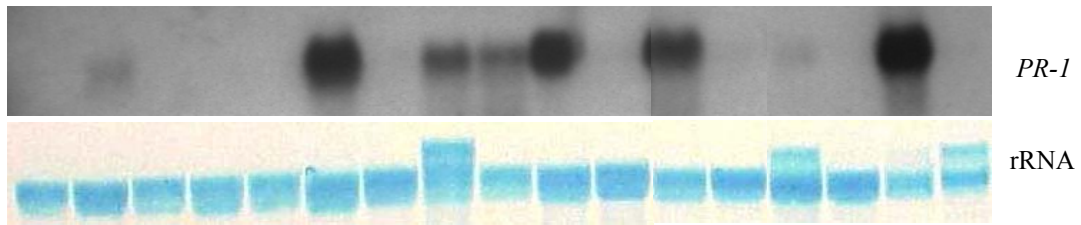


Figure 3-9. *PR-I* Northern hybridization. Numbers in the picture identify the days post-inoculation. I and U represent the inoculated and uninoculated leaves, respectively. (3 – 3 dpi and 7 – 7 dpi).

The levels of *PR-I* induction observed in the inoculated Di-3 plants were generally undetectable or low, consistent with that observed in mock-inoculated leaves, suggesting that the induction may be due to the stress of inoculation.

Similar to that observed in wt-inoculated Di-17 plants, at an early stage of infection (3 dpi), *PR-I* was rapidly induced in the D4E-inoculated leaves. Although a high level of *PR-I* was monitored at 7 dpi in the inoculated leaves, no obvious induction was detected in the asymptomatic uninoculated leaves.

D4S inoculated Di-3 and Di-17 plants displayed the relatively high levels of *PR-I* mRNA at 7 dpi in the inoculated leaves. The levels in Di-3 and Di-17 plants were similar. Surprisingly, these plants were lack of HR and displayed a resistance-

breaking phenotype. This increase was not due to more amount of RNA loaded on the gel. It suggests that this *PR-1* induction may reflect stress conditions rather than SAR-dependent expression.

In summary, rapid and strong induction of *PR-1* was observed in the wt TCV and D4E inoculated Di-17 plants – the plants that displayed resistance, i.e., HR and absence of systemic infection. In contrast, systemically infected plants, inoculated with D4N or D4S, displayed absent, weak or delayed and localized induction of *PR-1*.

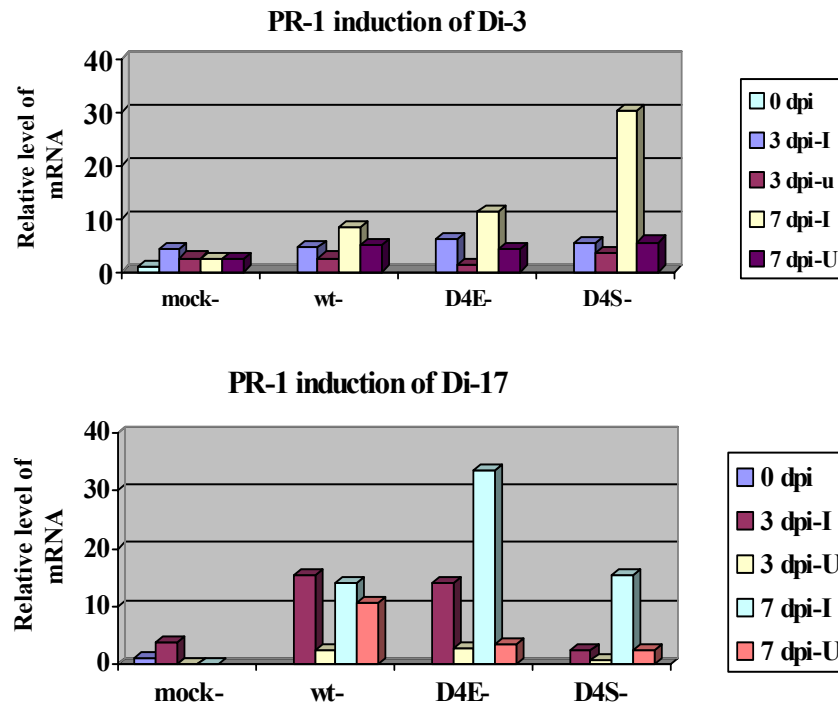


Figure 3-10. Relative levels of *PR-1* mRNA on TCV-inoculated *A. thaliana* plants. I and U shown above stand for the inoculated and uninoculated leaves.

These results from phenotype observation, viral RNA accumulation detection and *PR-1* induction monitoring indicate the different behaviors of D4E and D4S. These two mutations are both single mutations at amino acid four of TCV CP. The only difference between the mutations is the amino acid that replaces aspartate, which subsequently resulted in different phenotypes and molecular characteristics. TCV with D→E substitution maintains the ability to induce the HR and to induce *PR-1* activation locally; whereas D→S mutation is able to break resistance. Biochemical characteristics of amino acids that constitute the interacting domains, including hydrogen bonding, charges on side chains or hydrophilicity / hydrophobicity affect proteins interaction. In *Bacillus amuloliquefaciens*, for instance, Arg-59 residue in barnase (RNase) forms a salt bridge with Glu-76 in barstar, directly involved in barstar's ability to inhibit barnase. The R59E mutation prevented barstar-barnase interaction, however, which could be partially compensated by E76R mutation in barstar. Interchange of the charge in the two positions restored interaction (Jucovic *et al*, 1996).

Compared to aspartate, glutamate maintains the negative charge with one more methyl group in the side chain; whereas serine is a neutral, strong hydrogen bonding amino acid with approximately the same size as aspartate. Presumably, the D4E mutated CP could efficiently interact with the R protein in Di-17 plants, consequently activating the HR and SAR. Neutrality at amino acid four does not allow the CP to be recognized by the R protein, or reduction in affinity of the D4S

CP for the R protein produces an interaction too short-lived to trigger a strong resistance response.

Along with random mutagenesis, site – directed mutagenesis approach to producing D4E, D4S, K9E as well as D4N allows us to identify which amino acid is required and which domain is important, in terms of TCV-induced resistance. And meanwhile, it provides information about which precise chemical property of the amino acid determines CP recognition in TCV – *A. thaliana* model. Taken together, molecular analysis of resistance-breaking strains of TCV indicates that the CP of TCV is the key component in the “gene-for-gene” resistance pathway. The N-terminal sequence of the CP appears to be the sole recognition element to interact with the R protein in *A. thaliana*; a single mutation in this portion is sufficient to abrogate the interaction. Moreover, a negative charge at the fourth amino acid of the CP is required for CP recognition by the *R* gene product in *A. thaliana*.

3.2 DETECTION OF INTERACTIONS BETWEEN D4N MUTANT COAT PROTEIN AND *ARABIDOPSIS* TIP

D4N TCV had previously been demonstrated to elicit lesions, but not resistance on Di-3 plants, accompanied with *PR-1* induction and strong autofluorescence at the sites of macroscopic lesions. The delayed HR-like lesion was not observed in a similar inoculation of Di-17 plants (DelGrosso, 2000). TIP-CP interaction is suggested to be involved in induction of resistance (Ren *et al*, 2000).

Sequence analysis demonstrated several differences between the Di-3 TIP and the Di-17 TIP (Hammond and Souret, WPI). We were interested whether there was an interaction between the Di-3 TIP and the D4N CP that might be responsible for induction of the delayed HR in the D4N-inoculated Di-3 plants.

3.21 Analysis of variable infection patterns by D4N

3.21-1 Lack of HR-like lesion formation is possibly due to satellite RNA-C

To recapitulate the delayed HR-like lesion, *in vivo* D4N was used to inoculate Di-3 and Di-17 plants. All of D4N-inoculated plants became systemically diseased at 3 – 4 dpi. The plants developed a distinctive phenotype, with remarkably crinkled inner leaves (Figure 3-11). However, after observation (14 dpi), no HR-like lesion formation was observed on either Di-3 or Di-17 plants. Similarly, the levels of *PR-1* induction ranged from undetectable to low, consistent with the systemically infected phenotype (Figure 3-12). This D4N virus presented a different phenotype and plant response than had been previously observed (DelGrosso, 2000).

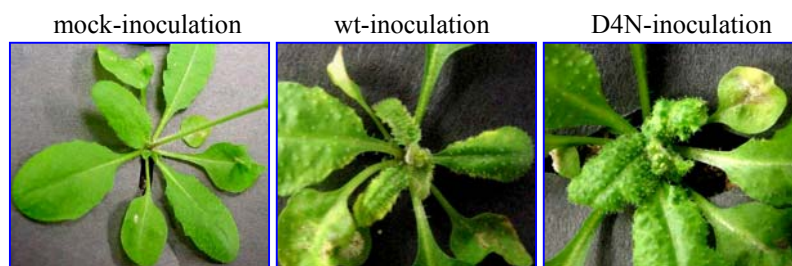
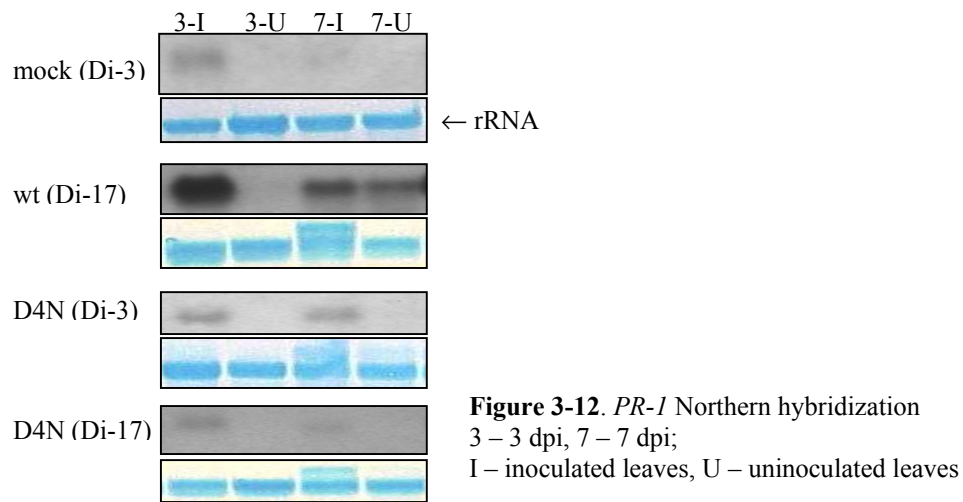


Figure 3-11. Distinctive phenotype developed in D4N-inoculated Di-3 plant at 9 dpi.



Formaldehyde gel analysis demonstrated the presence of a small RNA that correlated with viral infection and was the appropriate size to be a satellite RNA (Figure 3-13). Sat RNAs are small plant parasitic viral RNAs dependent on the function of a helper virus for replication, encapsidation and systemic movement (Collmer *et al*, 1992), sharing limited or partial sequence similarity with their helper viruses (Kong *et al*, 1997). Sat C, D and F are usually associated with TCV. Sat C, about 353-356 bases, intensifies wt TCV-induced symptoms, especially crinkling

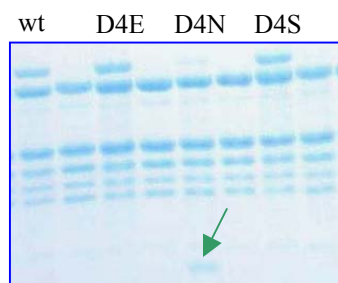


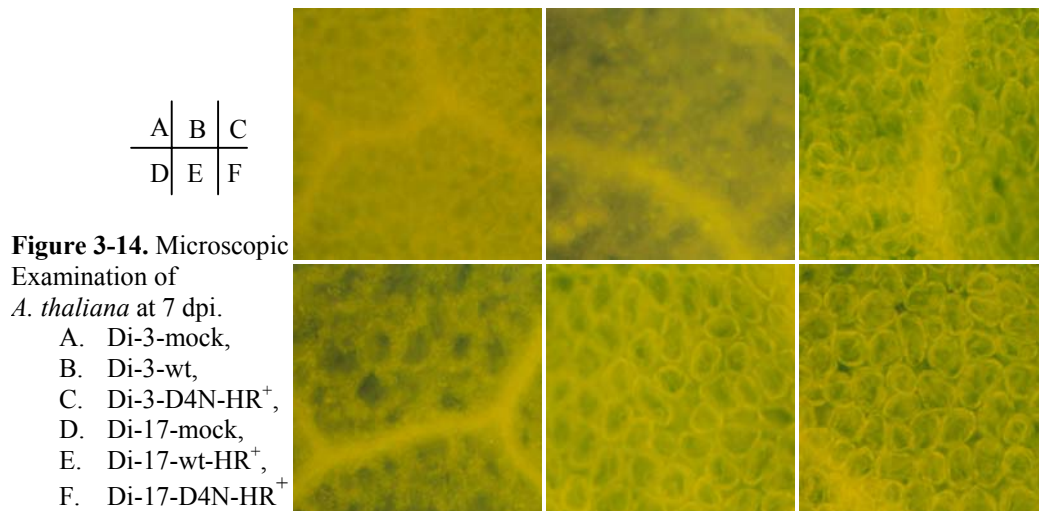
Figure 3-13. Methylene blue stain
of Northern transfer membrane

and stunting on all susceptible host plants (Collmer *et al*, 1992; Wang *et al*, 1999). According to the size on the gel and the phenotype induced by D4N, the additional RNA may be sat C. The involvement of sat RNA may be responsible for the distinctive phenotype observed after D4N inoculation, which may mask or compromise the infection pattern induced by D4N TCV alone.

3.21-2 Induction of the delayed HR-like lesions on both plants

It was desirable to use D4N virus without the extra RNA for inoculation. Analysis of another D4N stock revealed no small RNA contamination. After inoculation, D4N induced resistance-breaking in Di-17 plants. Unexpectedly, the HR-like lesion formation was not only observed in the inoculated Di-3 leaves, but also in the inoculated Di-17 leaves, two days later than HR occurrence in wt-inoculated Di-17. Unfortunately, due to the chlorosis of the inoculated leaves, it was difficult to take clear photos.

The inoculated leaves with or without HR-like lesion were easily distinguished by fluorescence microscopy (Figure 3-14). Plant tissue with lesion fluoresces quite brightly under UV light, while non-lesion tissue does not. Clear fluorescence was observed around cell walls on Di-17 leaves inoculated with wt TCV and D4N. Di-3 leaves inoculated with D4N but not wt TCV also fluoresced at lesion sites. Stronger autofluorescence made the cells undergoing HR sharper under the microscope.



PR-1 mRNA analysis was consistent with the phenotype. High levels of *PR-1* induction were monitored in the inoculated lesion-bearing leaves in Di-3 and Di-17 plants at 3 dpi, and sustained up to 7 dpi (Figure 3-15). However, the absence or low levels of *PR-1* induction were observed in the uninoculated leaves at 7 dpi, suggesting that the lack of systemic resistance contributes to generalized infection after D4N inoculation.

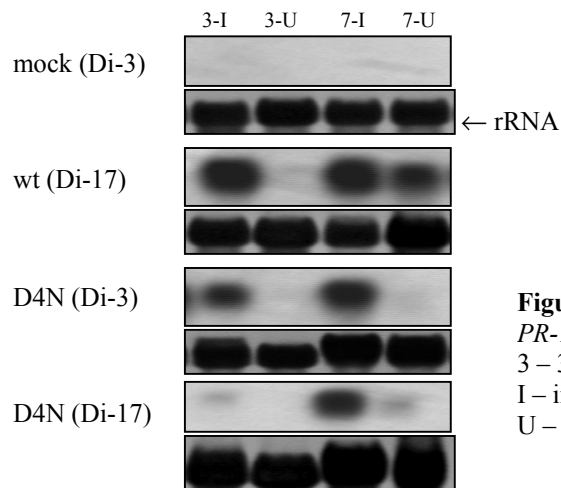


Figure 3-15. Northern hybridization for *PR-1* induction after D4N inoculation. 3 – 3 dpi, 7 – 7 dpi; I – inoculated leaves, U – uninoculated leaves

3.21-3 Absence of HR-like lesion formation upon *in vitro* D4N inoculation

Inoculation with different sources of *in vivo* D4N failed to recapitulate the phenotype reported by DelGrosso (2000). It was necessary to inoculate plant with *in vitro* D4N virus that was directly transcribed from D4N DNA. After inoculation, Di-3 and Di-17 plants exhibited systemic symptoms at 6-7 dpi. But, no lesion formation was observed up to 18 dpi. Northern hybridization was carried out to check if *PR-1* induction was correlated with the phenotype. Northern blot indicated the similar *PR-1* induction pattern presented by the inoculated Di-3 and Di-17 plants (Figure 3-16): the high levels of *PR-1* were detected in the inoculated leaves at 9 dpi, and the uninoculated leaves also showed low levels of induction at this time. The lack of systemic induction of *PR-1* (up to 9 dpi) was basically coincident with the systemically infected phenotype. It is possible that the lack of lesions may be due to the infection efficiency of *in vitro* RNA, which is usually 10 times less efficient than *in vivo* one (Wobbe, unpublished data). Alternatively, *in vitro* RNA may not be as stable as *in vivo* type, because the sequences at the ends are not identical to the *in vivo* produced RNA. To obtain an equivalent infection load as with *in vivo* RNA,

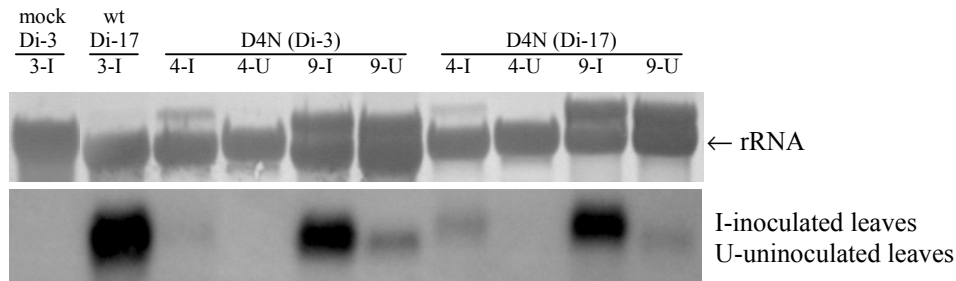


Figure 3-16. Northern hybridization for *PR-1* after *in vitro* D4N inoculation.

more *in vitro* RNA should be used and long-term observation is helpful.

The series of observations of various D4N inoculations in *A. thaliana* are summarized in Table 3-3. These different phenotypes are possible, because typically virus is produced first by synthesizing infectious RNA *in vitro*. This RNA is substantially less effective than RNA produced *in vivo*. Thus, the *in vitro* RNA is inoculated onto susceptible plants and infectious RNA is harvested after the plant begins to display systemic symptoms. Typically, the virus produced this way maintains fidelity to the original molecule. D4N appears to have a very high mutation rate such that the bulk of infectious RNA harvested has sustained some mutations.

Table 3-3. Variable infection patterns of D4N

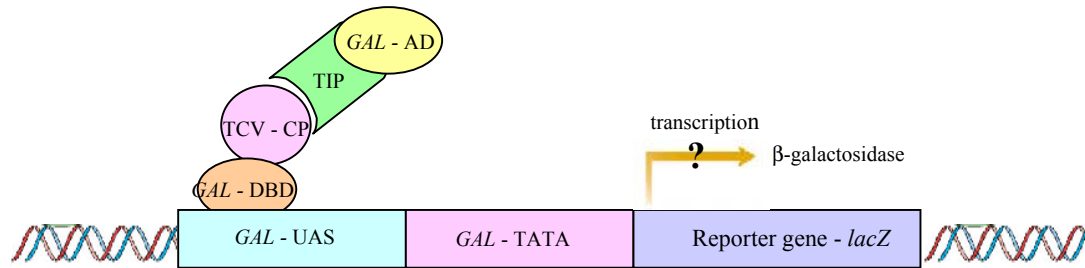
Feature of D4N	Phenotype in Di-3 and Di-17	<i>PR-I</i> induction
<i>in vivo</i> (turnip)	Systemic infection, lesions only on Di-3	Increase in Di-3 (DelGrosso, 2000)
<i>in vivo</i> with sat C (?)	Systemic infection, no lesions formation	Absent or low
<i>in vivo</i> (<i>A. thaliana</i>)	Systemic infection, lesions on Di-3 and Di-17	Rapid, high

3.22 Detection of the interaction between D4N CP and TIP

Since previous study had observed the delayed HR in D4N-inoculated Di-3 plants, it suggested that the mutated CP is recognized by its effector in Di-3, to some extent. We were interested in whether the D4N CP has a relatively higher binding affinity for Di-3 TIP than for Di-17 TIP. Therefore, as had previously been done for

detecting the CP – TIP interaction, a yeast two-hybrid assay (Figure 3-17) was carried out. This assay is a powerful tool to detect the possible interaction of two proteins (Pandey and Mann, 2000).

Figure 3-17. The principle of the yeast two-hybrid assay



The protein encoding sequence of wt TCV CP or D4N CP was cloned and inserted between *EcoRI* and *BamHI* sites of the DNA-binding domain (DBD) plasmid pGBT9, named wt-pGBT9 and D4N-pGBT9, respectively. The entire encoding region of Di-3 TIP or Di-17 TIP was cloned and inserted between *BamHI* and *PstI* sites of the activation domain (AD) plasmid pGAD424, named Di3-pGAD424 and Di17-pGAD424, respectively. The features of the plasmids used in the two-hybrid system are indicated in Table 3-4.

The yeast host strain Y187 was used for transformation, which contains *lacZ* as the reporter gene. Before starting transformations, the nutritional requirement phenotypes of Y187 were verified, i.e., Y187 cells only survived in the selectable medium with supplementary leucine and tryptophan. *GAL*-DBD and *GAL*-AD yeast plasmids were transformed simultaneously into Y187 cells. Each co-transformant

was placed on three types of selectable medium: 1) lacking Leu alone; 2) lacking Trp alone and 3) lacking both Leu and Trp.

Table 3-4. Description of the plasmids used in the yeast two-hybrid system

Plasmid	Size	Description	Yeast Selection	Bacterial Selection	Functions
pGBT9	5.4kb	<i>GAL4</i> ₍₁₋₁₄₇₎ DNA-bind domain	<i>TRP1</i>	<i>amp^r</i>	CP cloning plasmid
pGAD424	6.6kb	<i>GAL4</i> ₍₇₆₈₋₈₈₁₎ activation domain	<i>LEU2</i>	<i>amp^r</i>	TIP cloning plasmid
pCL1	15.3kb	wt full-length <i>GAL4</i> gene	<i>LEU2</i>	<i>amp^r</i>	positive control plasmid
pVA3	6.4kb	murine p53/ <i>GAL4</i> DBD hybrid in pGBT9	<i>TRP1</i>	<i>amp^r</i>	positive control plasmid
pTD1	15kb	SV40 large T-antigen/ <i>GAL4</i> AD hybrid in pGAD3F	<i>LEU2</i>	<i>amp^r</i>	positive control plasmid

β -galactosidase activity was assayed when the co-transformants (colonies) on the appropriate selectable medium grew to a diameter of > 2.0 mm. If the two hybrid proteins are interacting, the β -galactosidase assay will give a positive result: the colonies will turn blue on X-gal filter (Figure 3-18). All results of β -galactosidase assay of co-transformations with various combinations of the plasmids are shown in Table 3-5:

Figure 3-18. Positive β -gal assay shown by pVA3 and pTD1 co-transformation

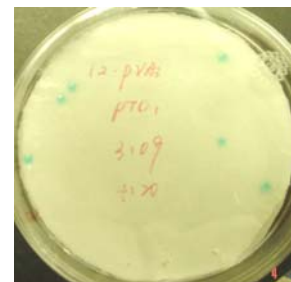


Table 3-5. Results of β -galactosidase assay [*: (+)- growth, (-)- no growth]

DBD plasmid	AD plasmid	Growth on selectable medium (-)Leu (-)Trp (-)Leu and Trp			Results of β -gal assay (colony color)	Function
pCL1	–	+	–	–	blue	positive control
pVA3	pTD1	+	+	+	blue	positive control
pVA3	–	–	+	–	white	negative control
–	pTD1	+	–	–	white	negative control
wt-pGBT9	–	–	+	–	white	negative control
D4N-pGBT9	–	–	+	–	white	negative control
–	Di3-pGAD424	+	–	–	white	negative control
–	Di17-pGAD424	+	–	–	white	negative control
pVA3	Di3-pGAD424	+	+	+	white	negative control
pVA3	Di17-pGAD424	+	+	+	white	negative control
wt-pGBT9	pTD1	+	+	+	white	negative control
D4N-pGBT9	pTD1	+	+	+	white	negative control
wt-pGBT9	Di3-pGAD424	+	+	+	white	
D4N-pGBT9	Di3-pGAD424	+	+	+	white	
wt-pGBT9	Di17-pGAD424	+	+	+	white	
D4N-pGBT9	Di17-pGAD424	+	+	+	white	

The observed lack of interaction between the wt TCV CP and the Di-17 TIP did not coincide with another group's data (Ren *et al*, 2000). To check if the negative results were due to non-expression of cloned CP or TIP in the yeast plasmids, DNA sequencing was performed, focusing on the 5' junction of the cloned proteins. Partial sequencing data confirmed that no additional mutations were found at the 5' junction portion of each cloned protein, except the engineered ones for restriction site introduction. The sequences suggested that the desired chimeras should be properly expressed.

There are a number of possible explanations for the lack of CP-TIP interaction in the yeast two-hybrid assay (Ito *et al*, 2000; Ito *et al*, 2001). First, PCR products sometimes incorporate mutations that could abrogate interaction. The C-terminal domain of TIP was not sequenced; thus, it is not known whether there are mutations occurring within this portion. Complete DNA sequencing for the cloned CP and TIP will confirm if there are additional mutations that impede interaction.

Another possibility is unstable or low-level expression of the hybrid protein(s), which also results in false negative. Analysis of protein expression in yeast cell may be helpful to detect this possibility.

Some other factors might also contribute to failure to detect the interaction between Di-17 TIP and wt CP. Different plasmids and yeast strains were used and there may be strain specific differences in protein production, stability and reporter gene(s) sensitivity.

Although the interaction between the D4N CP and the Di-3 TIP has not yet been detected, the possibility of interaction cannot be excluded. Further experiments should be carried out, including improvement of PCR fidelity, use of different plasmids and a yeast host strain that had been proven to be capable of detecting CP-TIP interaction, or performance of Western using purified CP-specific (or TIP-specific) antibody to check if the hybrid protein is expressed in yeast cellular environment.

4. FUTURE WORK SUGGESTION

1. Confirmation of the presence of the sole Lys→Glu mutation

Although K9E mutation conferred the resistance-breaking phenotype, it's necessary to perform DNA sequencing to confirm the presence of the sole mutation engineered.

2. Investigation of biochemical characteristics of D4N

We didn't succeed in reproducing the delayed HR seen in Di-3 plants inoculated with D4N TCV. Sequencing of the various D4N isolates would reveal changes that are responsible for the different phenotypes. I think it would be an interesting project to investigate why D4N mutant is more liable to induce the variation than other mutations occurring in this position. Meanwhile, recovery of Col-0 younger leaves after D4N inoculation was observed (Vaitkunas, 2002). It appears that the Asp→Asn substitution not only induces resistance-breaking, but also confers additional biochemical characteristics. Using TCV *in situ* hybridization to compare viral accumulation pattern in the D4N-inoculated, uninoculated and newly growing leaves, could help explain why the Col-0 plants appear to produce healthy leaves after clearly demonstrating systemic disease.

3. Detection of the interaction between TCV CP and TIP

We failed to detect any interaction between TCV CP and *A. thaliana* TIP, but the possibility cannot be excluded. A Western blot to detect TCV CP or CP-TIP complex (directly detecting TIP if TIP-specific antibody is available) will find out if the hybrid protein(s) is stably expressed in the yeast environment. It's also worth trying a different yeast two-hybrid system (different yeast host strain and vectors) to detect the interaction. Alternatively, co-immunoprecipitation assay or other methods also can be used to detect possible interactions.

REFERENCES

- Agrios, G.N. (1988) How plants defend themselves against pathogens. In "Plant pathology" (third edition), pp.97-115. Academic Press, San Diego, New York, Berkeley, Boston, London, Sydney, Tokyo and Toronto.
- Akgoz, M., Drainville, K., Talmadge, A. and Wobbe, K.K. (2001) Mutational analysis of *Turnip crinkle virus* movement protein p8. *Mol. Plant Pathol.* **2**, 37-48
- The Arabidopsis Genome Initiative (2000). Analysis of the genome sequence of the flowering plant *Arabidopsis thaliana*. *Nature* **408**, 796-815
- Antoniw, J.F., Ritter, C.E. Pierpoint, W.S. and van Loon, L.C. (1980). Comparison of three pathogenesis-related proteins from plants of two cultivars of tobacco infected with TMV. *J. Gen. Virol.* **47**, 79-87
- Astua-Monge, G., Minsavage, G.V., Stall, R.E., Davis, M.J., Bonas, U. and Jones, J.B. (2000) Resistance of tomato and pepper to T3 strains of *Xanthomonas campestris* pv. *vesicatoria* is specified by a plant – inducible avirulence gene. *Mol. Plant Pathol.* **13**, 911-921
- Bustamante, P.I. and Hull, R. (1998) Plant virus gene expression strategies. *Electronic J. Biotech.* **2**
- Carrington, J.C., Heaton, L.A., Zuidema, D., Hillman, B.I., and Morris, T.J. (1989) The genome structure of turnip crinkle virus. *Virology* **170**, 219-225
- Collmer, C.W., Stenzler, L., Chen, X., Fay, N., Hacker, D. and Howell, S.H. (1992). Single amino acid change in the helicase domain of the putative RNA replicase of turnip crinkle virus alters symptom intensification by virulent satellites. *Proc. Natl. Acad. Sci. USA* **89**, 309-313
- Culver, J.N., Stubbs, G. and Dawson, W.O. (1994). Structure-function Relationship Between Tobacco Mosaic Virus Coat Protein and Hypersensitivity in *Nicotiana sylvestris*. *J. Mol. Biol.* **242**, 130-138
- Dangl, J.L. and Jones, D.G. (2001) Plant pathogens and integrated defence responses to infection. *Nature* **411**, 826-833
- DelGrosso, J.L. (2000). Characterization of resistance-breaking strains of *Turnip crinkle virus*. M.S. thesis, WPI

- Dempsey, D.A., Wobbe, K.K. and Klessig, D.F. (1993). Resistance and susceptible responses of *Arabidopsis thaliana* to Turnip crinkle virus. *Phytopathol.* **83**, 1021-1029
- Dempsey, D.A., Pathirana, M.S., Wobbe, K.K. and Klessig, D.F. (1997). Identification of an *Arabidopsis* locus required for resistance to turnip crinkle virus. *Plant J.* **11**(2), 301-311
- Eddins, G.K. (2000). Biochemical characterization of a protein-protein interaction. MQP, WPI.
- Ellis, J.G., Lawrence, G.J., Luck, J.E. and Dodds, P.N. (1999). Identification of regions in alleles of the flax rust resistance gene *L* that determine differences in gene-for-gene specificity. *Plant Cell* **11**, 495-506
- Flor, H. (1971) Current status of the gene-for-gene concept. *Annu. Rev. Phytopathol.* **9**, 275-296
- Glazebrook, J., Rogers, E.E. and Ausubel, F.M. (1997). Use of *Arabidopsis* for genetic dissection of plant defense responses. *Annu. Rev. Genet.* **31**, 547-569
- Hacker, D.L., Petty, I.T.D., Wei, N., and Morris, T.J. (1992) Turnip crinkle virus genes required for replication and movement. *Virology* **186**, 1-8
- Heaton, L.A., Carrington, J.C. and Morris, T.J. (1989). Turnip crinkle virus infection with RNA synthesized *in vitro*. *Virology*, **170**, 214-218
- Heaton, L.A., Lee, T.C., Wei, N. and Morris, T.J. (1991). Point mutations in the turnip crinkle virus capsid protein affected the symptoms expressed by *Nicotiana benthamiana*. *Virology* **183**, 143-150
- Hogel, J.M., Maede, A., and Harrison, S.C. (1986) Structure and assembly of turnip crinkle virus. I. X-ray crystallographic structure analysis at 3.2Å resolution. *J. Mol. Biol.* **191**, 625-638
- Hammond-Kosack, K.E. and Jones, J.D.G. (1997) Plant disease resistance genes. *Annu. Rev. Plant Physiol. Plant Mol. Biol.* **48**, 575-607
- Hammond, T.M. (2001). *Turnip crinkle virus* and the suppression of the hypersensitive response. MS thesis, WPI.
- Ito, T., Tashiro, K., Muta, S., Ozawa, R., Chiba, T., Nishizawa, M., Yamamoto, K., Kuhara, S. and Sakaki, Y. (2000). Toward a protein-protein interaction map of the budding yeast: A comprehensive system to examine two-hybrid interactions in all

possible combinations between the yeast proteins. *Proc. Natl. Acad. Sci. USA* **97**, 1143-1147

Ito, T., Chiba, T., Ozawa, R., Yoshida, M., Hattori, M. and Sakaki, Y. (2001). A comprehensive two-hybrid analysis to explore the yeast protein interactome. *Proc. Natl. Acad. Sci. USA* **98**, 4569-4574

Jia, Y., McAdams, S.A., Bryan, G.T., Hershey, H.P. and Valent, B. (2000). Direct interaction of resistance gene and avirulence gene products confers rice blast resistance. *EMBO J.* **19**, 4004-4014

Joosten, M.H., Cozijnsen, T.J., and De Wit, P.J. (1994) Host resistance to a fungal tomato pathogen lost by a single base-pair change in an avirulence gene. *Nature* **367**, 384-386

Jucovic, M. and Hartley, R.W. (1996) Protein-protein interaction: A genetic selection for compensating mutations at the barnase-barstar interface. *Proc. Natl. Acad. Sci. USA* **93**, 2343-2347

Kobe, B and Deisenhofer, J. (1994) The leucine – rich repeat: a versatile binding motif. *Trends Biochem. Sci.* **19**, 415-21

Kong, Q., Oh, J-W., Carpenter, C.D. and Simon, A.E. (1997). The coat protein of turnip crinkle virus is involved in subviral RNA-mediated symptom modulation and accumulation. *Virology* **238**, 478-485

Lucas, J.A. (1998). Plant pathology and plant pathogens. Third Edition. Blackwell Science

Matin, G.B., Frary, A., Wu, T., Brommonschenkel, S., Chunwongse, J., Earle, E.D., and Tanksley, S.D. (1993) A member of the tomato Pto gene family confers sensitivity to fenthion resulting in rapid cell death. *Plant Cell* **6**, 1543-1552

Mohr, P.G. and Cahill, D.M. (2000). Relative roles of glyceollin, lignin and the hypersensitive response and the influence of ABA in compatible and incompatible interactions of soybeans with *Phytophthora sojae*. *Physiol. Mol. Plant Pathol.* **58**, 31-41

Pandey, A. and Mann, M. (2000). Proteomics to study genes and genomes. *Nature* **405**, 837-846

- Ren, T., Qu, F. and Morris, T.J. (2000) *HRT* gene function requires interaction between a NAC protein and viral capsid protein to confer resistance to turnip crinkle virus. *Plant Cell* **12**, 1917-1925
- Ren, T., Qu, F. and Morris, T.J. (2001). Characterization of functional domains of a NAC protein involved in conferring resistance in *Arabidopsis* to *turnip crinkle virus*. *American Society for Virology, 20th annual meeting* Poster P43-3
- Saraste, M., Sibbald, P.R. and Wittinghofer, A. (1990). The p--loop: a common motif in atp- and gtp-binding proteins. *Trends in Biochem.* **15**,430-434
- Scofield, S.R., Tobias, C.M., Rathjen, J.P., Chang, J.H., Lavelle, D.T., Michelmore, R.W. and Staskawicz, B.J. (1996). Molecular basis of gene-for-gene specificity in bacterial speck disease of tomato. *Science* **274**, 2063-2065
- Shan, B., Thara, V.K., Martin, G.B., Zhou, J-M. and Tang, X. (2000). The *Pseudomonas* AvrPto protein is differentially recognized by tomato and tobacco and is localized to the plant plasma membrane. *Plant Cell* **12**, 2323-2337
- Soger, P.K., Stockley, P.G., and Harrison, S.C. (1986) Structure and assembly of turnip crinkle virus. II. Mechanism of reassembly *in vitro*. *J. Mol. Biol.* **191**, 639-658
- Tang, X., Frederick, R.D., Zhou, J., Halterman, D.A., Jia, Y., and Martin, G.B. (1996) initiation of plant disease resistance by physical interaction of avrPto and Pto kinase. *Science* **274**, 2060-2063
- Thomas, C.M., Jones, D.A., Parniske, M., Harrison, K., Balint-Kurti, P.J., Hatzixanthis, K. and Jones, J.D. (1997). Characterization of the tomato Cf-4 gene for resistance to *Cladosporium fulvum* identifies sequences that determine recognitional specificity in Cf-4 and Cf-9. *Plant Cell* **9**, 2209-2224
- Traut, T.W. (1994). The functions and consensus motifs of nine types of peptide segments that form different types of nucleotide-binding sites. *Eur. J. Biochem.* **222**, 9-19.
- Vaikunas, K. (2002). Genetics of *Turnip crinkle virus* resistance. MQP, WPI
- van der Biezen, E.A. and Jones, J.D.G. (1998) Plant disease resistance proteins and the “gene-for-gene” concept. *Trends Biochem.* **23**, 454-456
- van Loon, L.C. (1982) Regulation of changes in proteins and enzymes associated with active defense against virus infection. In: Active defense mechanisms in plants (R.K.S. Wood, ed.), pp.247-273, Plenum Press, New York, USA.

van Loon, L.C. (1997) Induced resistance in plants and the role of pathogenesis-related proteins. *Eur. J. Plant Pathol.* **103**, 753-765

van Loon, L.C. and van Strien E.A. (1999). The families of pathogenesis-related proteins, their activities, and comparative analysis of PR-1 type proteins. *Physiol. Mol. Plant Pathol.* **55**, 85-97

van Wees, S.C.M., de Swart, E.A.M., van Pelt, J.A., van Loon, L.C. and Pieterse, C.M.J. (2000). Enhancement of induced disease resistance by simultaneous activation of salicylate- and jasmonate-dependent defense pathways in *Arabidopsis thaliana*. *Proc. Natl. Acad. Sci. USA* **97**, 8711-8716

Wang, J-L. and Simon, A.E. (1999) Symptom attenuation by a satellite RNA *in vivo* is dependent in reduced levels of virus coat protein. *Virology* **259**, 234-245

White, K.A., Skuzeshi, J.M., Li, W., Wei, N., and Morris, T.J. (1995) Immunodetection, expression strategy and complementation of turnip crinkle virus p28 and p88 replication components. *Virology* **211**, 525-534

Wong, C.E., Carson, R.A.J., and Carr, J.P. (2002) Chemically induced virus resistance in *Arabidopsis thaliana* is independent of pathogenesis-related protein expression and the *NPR1* gene. *Mol. Plant-Microbe Interact.* **15**, 75-81

Yalpanin N., Altier, D.J., Barbour, E., Cigan, A.L. and Scelonge, C.J. (2001). Production of 6-methylsalicylic acid by expression of a fungal polyketide synthase activates disease resistance in tobacco. *Plant Cell* **13**, 4001-4010.

Zhao, Y-J., DelGrosso, L., Yigit, E., Dempsey, D.M., Klessig, D.F. and Wobbe, K.K. (2000) The amino terminus of the coat protein of turnip crinkle virus is the AVR factor recognized by resistant *Arabidopsis*. *Mol. Plant-Microbe Interact.* **13**, 1015-1018